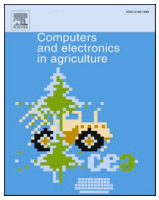
Computers and Electronics in Agriculture 227 (2024) 109603



Contents lists available at ScienceDirect

Computers and Electronics in Agriculture

journal homepage: www.elsevier.com/locate/compag





Upscaling and downscaling approaches for early season rice yield prediction using Sentinel-2 and machine learning for precision nitrogen fertilisation

Giorgio Impollonia *, Michele Croci, Stefano Amaducci

Department of Sustainable Crop Production, Università Cattolica del Sacro Cuore, Piacenza 29122, Italy
Remote Sensing and Spatial Analysis Research Center (CRAST), Università Cattolica del Sacro Cuore, 29122 Piacenza, Italy

ARTICLE INFO

Keywords:
Precision agriculture
Within-field variability
Satellite
Yield prediction
Transferability

ABSTRACT

Early season yield prediction could support rice farmers in adopting precision agriculture for nitrogen fertilisation management. Remote sensing and machine learning (ML) can be used to predict and map crop yield during phenological stages relevant to nitrogen application, like tillering in rice, at both within-field and field scales. This study evaluated the transferability of ML models in early season yield prediction through upscaling and downscaling approaches. The effects of two prediction times (tillering and ripening stages) and training/testing set sizes on ML models performance were evaluated over five rice growing seasons (from 2018 to 2022) in northern Italy, using whole-field-average yields and yield maps. Vegetation indices from Sentinel-2 imagery using the Google Earth Engine platform fed five ML algorithms (Cubist-CUB, Gaussian Process Regression-GPR, Neural Network-NNET, Random Forest-RF, and Support Vector Machines-SVM). ML algorithms were trained with yield maps and tested with whole-field-average yields to obtain a downscaling approach, while the opposite was done to obtain an upscaling approach. The downscaling approach showed higher accuracy than upscaling approach. Ripening stage predictions were more accurate than tillering stages, although the downscaling approach showed small differences between tillering and ripening stages. The highest tillering stage accuracy was achieved by SVM for both downscaling and upscaling approaches with 20 % and 27.8 % of Normalized Root Mean Square Error (NRMSE), and 0.99 and 0.99 of Simple Additive Weighting (SAW) score, respectively. Set size and data distribution effected ML models accuracy, with the highest performance achieved by RF and GPR with 0.80 and 1.00 of SAW score for the downscaling and upscaling approaches, respectively. This study demonstrated how ML models and downscaling approach could support rice farmers to calculate the nitrogen dose using the predicted yield at the tillering stage, enabling them to apply a site-specific nitrogen fertilisation based on the within-field yield prediction variability.

1. Introduction

Agricultural production must keep pace with the ever-increasing global demand for food to ensure food security in the future (Gerten et al., 2020; van Dijk et al., 2021). The potential impact of climate change on future crop yields is a major concern for society (Jägermeyr et al., 2021). Climate change yield effects are well documented in several field crops (Asseng et al., 2013; Bassu et al., 2021; Cammarano et al., 2021, 2019; Guarin et al., 2022; Hasegawa et al., 2022; Liu et al., 2019; Yu et al., 2022). Future climate projections indicate that Mediterranean countries will become drier and hotter, potentially leading to severe yield reductions (Cammarano et al., 2019; Senapati et al., 2019). The north-west of Italy area, which is the largest area for rice production in Italy and in Europe (Arcieri and Ghinassi, 2020), is considered a hotspot regarding climate change. Indeed, drought has particularly affected it in recent years (Caloiero et al., 2021), leading to rice yields falling by more than 30 % (Coldiretti, 2022). In fact, rice fields will be the agricultural system most affected by climate change in northern Italy (Straffelini and Tarolli, 2023).

Agricultural systems contribute to human-induced global warming, and reducing emissions from agriculture can be an important part of climate change mitigation (Lynch et al., 2021). In response to climate change's impact, advanced agricultural technologies have been adopted as a global trend (Lybbert and Sumner, 2012). Precision agriculture has

* Corresponding author.
E-mail address: giorgio.impollonia@unicatt.it (G. Impollonia).

https://doi.org/10.1016/j.compag.2024.109603
Received 21 March 2024; Received in revised form 7 October 2024; Accepted 27 October 2024
Available online 3 November 2024
0168-1699/© 2024 The Authors. Published by Elsevier B.V. This is an open access article under the CC BY license (http://creativecommons.org/licenses/by/4.0/).

been identified as an effective way to mitigate the impact of agricultural systems on the environment (Roy et al., 2020). Precision agriculture uses advanced technologies such as satellite imagery and yield maps to monitor and predict crop yields, providing key information to improve agricultural management efficiency in decision-support systems (Bacenetti et al., 2020; Veerakachen and Raksapatcharawong, 2020). Spatio-temporal mapping of yield prediction is important for precision agriculture adoption, which aims at within-field variability management (Bouma, 2007). A reliable and early season yield prediction can help farmers to adopt suitable measures to improve crop yield through optimising agricultural inputs management (Jeong et al., 2022). For example, an early season rice yield prediction is important to support the farmers for topdressing nitrogen fertilisation dose calculation during the tillering and stem elongation phenological stages (Zhang et al., 2019). At the same time, a yield prediction at the end of the growing season is important to retrieve historical yield maps to evaluate the spatio-temporal yield variability and stability of crop fields (Adhikari et al., 2023; Maestrini and Basso, 2021). Yield prediction information is also essential for the agricultural food chain (e.g., individual producers, processing industries and regional authorities) and for supporting national and international food security policies (Kasampalis et al., 2018).

Remote sensing is a technology widely used for yield prediction both at a regional scale (Meroni et al., 2021; Stepanov et al., 2020) and at within-field variability (Croci et al., 2022b; Kayad et al., 2019). Satellite remote sensing (e.g., Sentinel-2) enables the acquisition of spectral information useful to derive vegetation indices (VIs) that are linked with crop yield traits such as leaf area index (Croci et al., 2022a). Several studies have used satellite imagery for the development of regional and field-scale rice monitoring systems (Busetto et al., 2017; Granell et al., 2017; Nutini et al., 2021; Ranghetti and Boschetti, 2022) and yield prediction (Ali et al., 2022; Basso and Liu, 2019; Liu et al., 2022).

Machine learning (ML) regression is a statistical method recognising nonlinear and nonparametric relationships between predictor and dependent variables. ML is widely used for rice yield prediction (Cao et al., 2021b; Lingwal et al., 2022; van Klompenburg et al., 2020) and several ML algorithms have been used such as random forest (Choudhary et al., 2022; Li et al., 2021), support vector machines (Son et al., 2020), gaussian process regression (Duque et al., 2023) and neural networks (Son et al., 2022). To achieve reliable and accurate yield predictions, it is crucial to have high-quality yield data for ML models. Data sources used for remotely sensed yield prediction are typically district-average and whole-field-average or yield maps, which are valuable for mapping spatio-temporal within-field yield variability (Whelan and Taylor, 2013). However, the transferability of ML models is one of the main limitations of their applications, which is often related to the size of the training set and the range of values of the parameters present in the training set (Impollonia et al., 2022b). In this context, no studies evaluated the ML transferability to predict crop yields using different data sources, like whole-field-average and yield maps, to train and test the ML models. This evaluation is interesting for upscaling and downscaling approaches using ML models for yield prediction for precision agriculture applications. For example, a yield prediction using upscaling approach could be used in the rice fields with low within-field variability, while downscaling approach could be used in rice fields with high within-field variability for site-specific nitrogen fertilisation application or for yield mapping in order to delineate yield stability zones using multi-year data. The evaluation and comparison of downscaling and upscaling approaches for yield prediction has not been addressed in other studies. However, it is a topic of great interest that needs to be investigated and explored in depth.

The main objective of this work was to obtain an early season prediction and to map the spatio-temporal rice yield using ML algorithms and remote sensing data, and to use the predicted yield to calculate the nitrogen dose to be applied in rice fields for precision and site-specific nitrogen fertilisation. Particular emphasis was placed on: i) evaluating the transferability of ML models in upscaling and downscaling approaches using two sources of yield data collected over three and five growing seasons, respectively of yield maps and of whole-field-average yields, ii) evaluating the effects of training and testing size on ML models performances, and iii) identifying the most suited ML algorithm for application purposes. Findings from this work could support rice farmers to adopt precision agriculture techniques for nitrogen fertilisation management.

2. Materials and methods

The workflow for rice yield prediction is based on three main steps including data pre-processing, data analysis, and data evaluation (Fig. 1). The data pre-processing step included yield data preparation, rice phenology estimation, and the calculation of vegetation indices (VIs). The data analysis step included machine learning modelling and validation. Finally, the data evaluation step included the calculation of model performance metrics.

2.1. Study area and data sources

The study area is located in northern Italy, in the province of Pavia, where rice production is highly specialised and concentrated. This area is characterised by loam and sandy-loam soil texture with neutral pH, and it has a temperate subcontinental climate (Kottek et al., 2006).

Twenty Italian rice cultivars, including 5 early, 8 intermediate and 7 late maturity types, were cultivated in the monitored fields. The rice fields were sown between 11 April and 25 May and were harvested between 09 September and 08 November over five growing seasons from 2018 to 2022. Rice fields information are reported in supplementary material Table S1.

Yield data were collected from 116 rice fields during five growing seasons, from 2018 to 2022. The area of the rice fields ranged from 0.51 ha to 9.31 ha, with an average of 3.55 ha. 238 whole-field-average yields were collected during the monitoring period and in particular 15, 5, 61, 77, and 80 yield data in 2018, 2019, 2020, 2021, and 2022 respectively (Fig. 2a). In addition, 70 yield maps were collected in 30 monitored fields using a GPS-equipped harvester, with 29, 24, and 17 yield maps in 2020, 2021, and 2022 respectively. Outliers were removed from the raw data of yield maps using the 1° and 99° percentiles of yield and based on the speed and swath width of machinery. Yield maps values were aggregated using the 20 m x 20 m grid of Sentinel-2 (Fig. 2c). A 20 m buffer was applied inside the field boundaries to avoid edge effects. After this step, the total number of Sentinel-2 pixels, within the yield map fields, was 3674. The average yield map data for each pixel was then calculated and 3674 yield data for yield maps source were obtained. The yield maps and whole-field-average yields data were converted to 14 % of moisture content and their distributions are reported in Fig. 2b and Fig. 2d. Details of the yield distribution between years are reported in supplementary material Table S2.

2.2. Weather data and phenological stage estimation

Weather data were downloaded from the meteorological station of the ARPA network (https://www.arpalombardia.it/) and are reported in supplementary material Table S3. The growing seasons considered in this study were characterised by large variations in temperature and rainfall; for example, 2022 had exceptionally low rainfall.

Weather data were used to estimate rice phenology. Phenological stages were expressed as thermal time, by estimating cumulative growing degree days (GDD, $\sum$ °C day^{-1}) from sowing to maturity as reported by Mongiano et al. (2020). Cumulative GDD were determined based on the daily average air temperature (T, °C) according to Weikai and Hunt (1999) as follows:

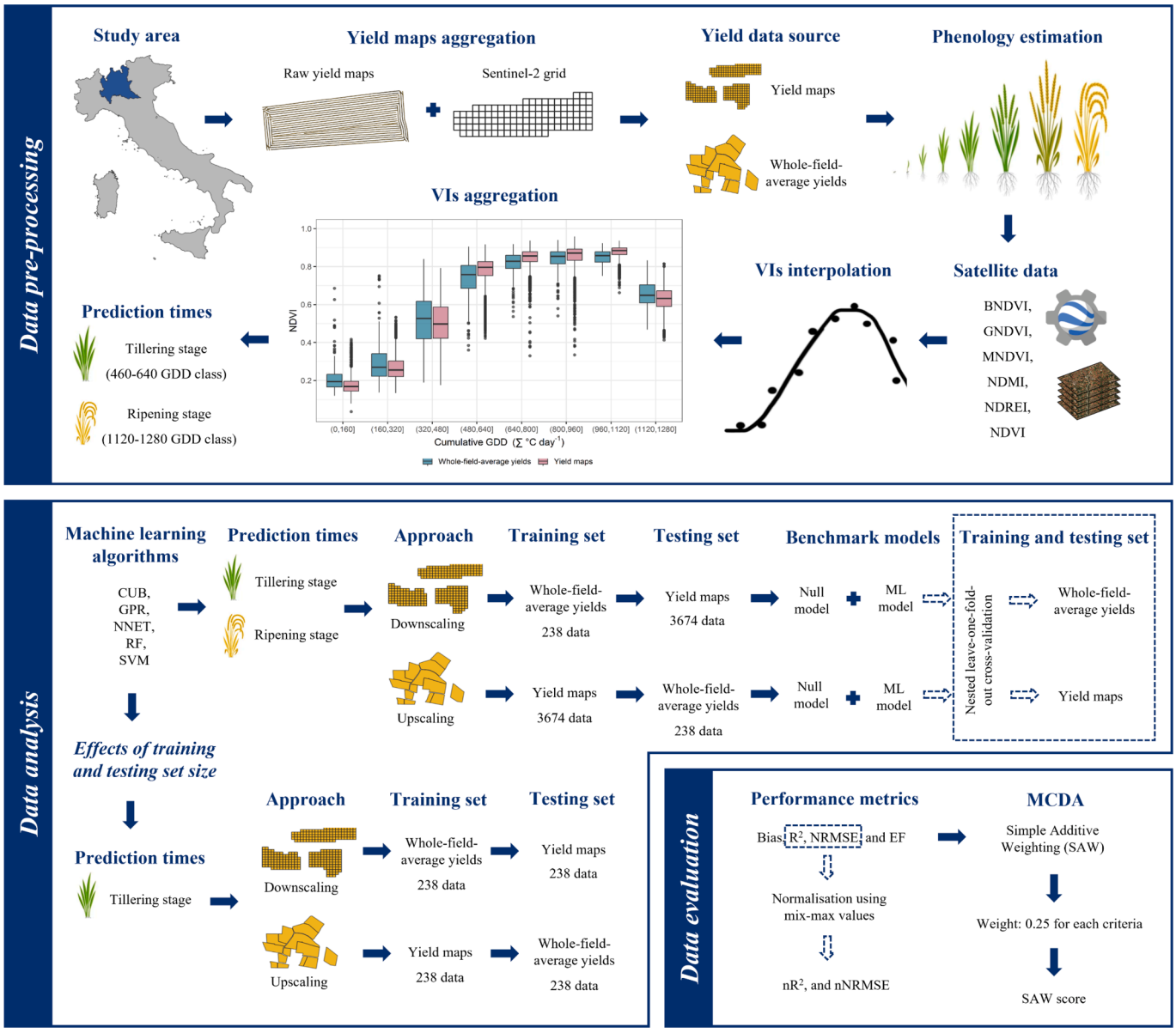


Fig. 1. The workflow of the study consisted of three main steps: data pre-processing, data analysis and data evaluation.

$$GDD = \left(T_{opt} - T_{min}\right) \times \frac{T_{max} - T}{T_{max} - T_{opt}} \times \left(\frac{T}{T_{opt}}\right)^{\frac{T_{opt}}{T_{max} - T_{opt}}}$$

where T_{min}, T_{opt}, and T_{max} are the minimum, optimum, and maximum cardinal temperatures (°C) for rice (sub-species *japonica*) development (Sánchez et al. (2014).The minimum, optimum, and maximum temperatures used were 13.5 °C, 28 °C, 36 °C from sowing to flowering and 20.7 °C, 24.2 °C, 31.3 °C from flowering to maturity, according to Sánchez et al. (2014). The cumulative GDD were divided into eight classes ranging from 0 to 1280 with intervals of 160 ($\sum$ °C day^{-1}). To determine the phenological stage of each cumulative GDD class, the days after sowing were calculated and compared with the days after sowing of the main phenological stages of rice (Fig. 3). Stem elongation is a crucial stage for nitrogen fertilisation in rice. Implementing precision agriculture techniques, through a proactive and early season yield prediction at tillering stage, i.e. before the onset of stem elongation stage, is fundamental to support the rice farmers for nitrogen fertilisation management. In this study, the cumulative GDD class between 480 and 640 ($\sum$ °C day^{-1}) was identified as a suitable cumulative GDD class for yield prediction at the tillering stage, which is sufficiently early for precision nitrogen fertilisation application.

2.3. Sentinel-2 data processing

Spectral information of rice fields were acquired using the cloud-based computing platform Google Earth Engine (GEE, Gorelick et al., 2017). Copernicus Sentinel-2 A and B satellite image processing and vegetation indices (VIs) calculation were performed using GEE 'eemont' module (Montero, 2021) and the 'awesome-spectral-indices' Python library for GEE (Montero et al., 2023). Sentinel-2 spectral bands were resampled at 20 m and six VIs were calculated: Blue Normalized Difference Vegetation Index (BNDVI, Wang et al., 2007), Green Normalized Difference Vegetation Index (GNDVI, Gitelson et al., 1996), Modified Normalized Difference Vegetation Index (MNDVI, Jurgens, 1997), Normalized Difference Moisture Index (NDMI, Wilson and Sader, 2002), Normalized Difference Red-Edge Index (NDREI, Gitelson and Merzlyak, 1994), and Normalized Difference Vegetation Index (NDVI, Rouse et al., 1974). The formulas used to calculate these VIs are reported in Table S4. These VIs have been widely used for yield prediction (Schauberger et al.,

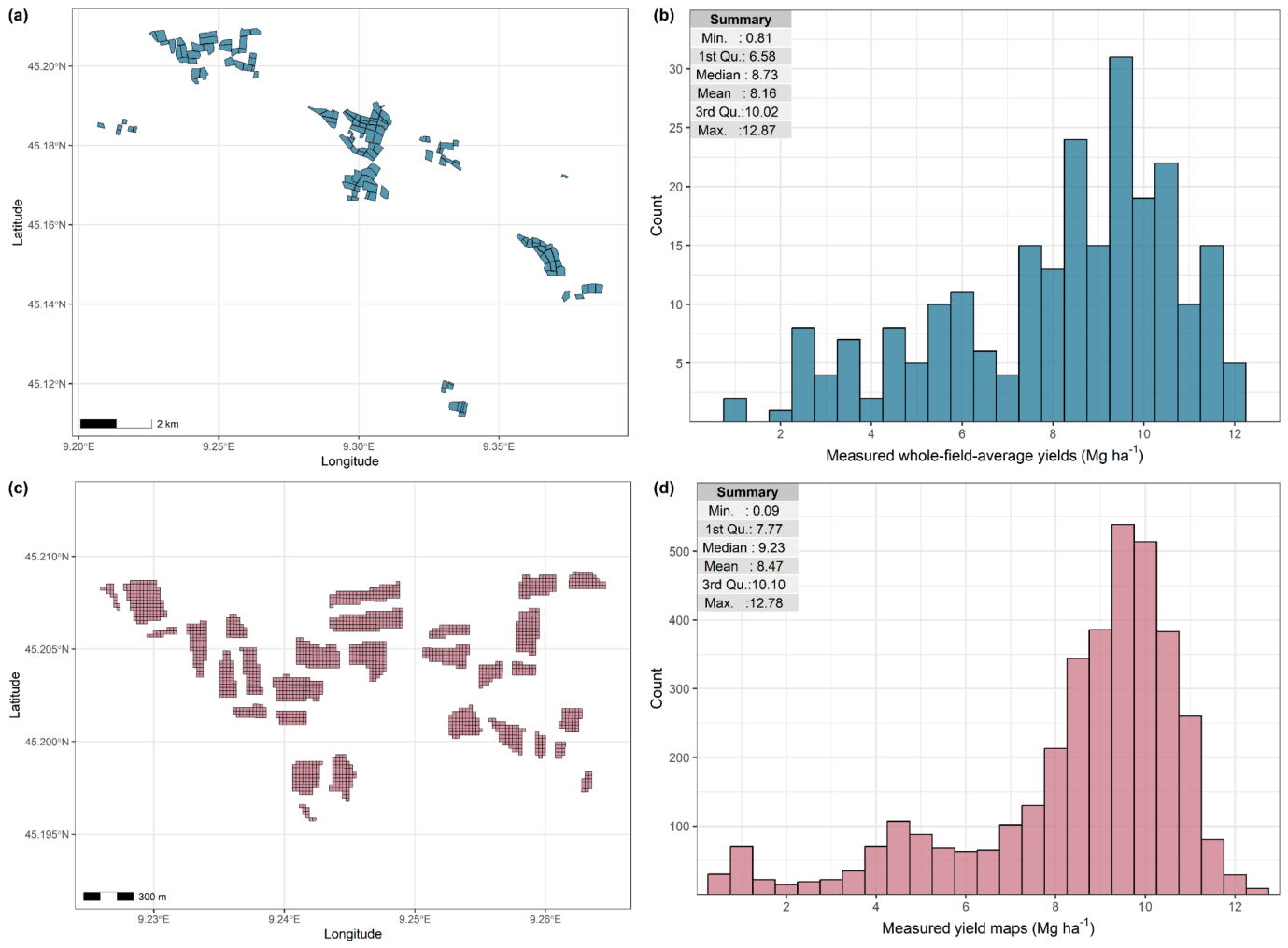


Fig. 2. Locations (a) and distributions (b) of the whole-field-average yields (Mg/ha). Locations (c) and distributions (d) of yield maps (Mg/ha) based on 20 m x 20 m Sentinel-2 grid.

2020). In the first step, all the available Sentinel-2 images (i.e. from 0 % to 100 % of cloud cover) between the dates of rice sowing and harvesting, during the five monitored growing seasons (2018, 2019, 2020, 2021, and 2022), were considered. In the second step, the VIs' time series were downloaded and subsequently filtered using the mean scene classification values between four and five (with decimal values also taken into account due to averaging). This approach enabled the extraction of clean VIs data without cloud interference, whereas using a specific cloud cover value as a filter could have resulted in the loss of some VIs data from certain rice fields. The VIs' time series were downloaded in two different approaches. The first approach consisted in downloading the mean value of the VIs' time series using the 20 m x 20 m Sentinel-2 grid used for the aggregation of the yield maps, while the second approach is based on the extraction of the mean value of the VIs' time series using the boundaries of the monitored fields. Stineman interpolation (Stineman, 1980)was used to reconstruct the daily time series of each VI. This method is particularly effective in preserving the integrity of observed trends in the time series, as it constrains interpolated values within the range of existing observations, ensuring alignment with the dataset's underlying trends (Vance et al., 2022). Furthermore, studies have demonstrated that Stineman interpolation is highly accurate and precise for imputing missing values (Demirhan and Renwick, 2018; Moknatian and Piasecki, 2019). After interpolation, the average value of the six vegetation indices (BNDVI, GNDVI, MNDVI, NDMI, NDREI, and NDVI) was calculated for each of the eight cumulative GDD classes evaluated in this study, as shown in Fig. 4.

2.4. Machine learning workflow

2.4.1. Prediction time and machine learning algorithms

Yield prediction was computed at two different times of the growing season: an early season prediction at tillering stage and a late prediction at ripening stage. Yield prediction at the ripening stage, i.e. at the end of the rice growing season, is used to evaluate the accuracy and performance of yield prediction models developed at the tillering stage, i.e. approximately 60 days after rice sowing. The yield prediction models used the six VIs generated from the start of the season until the cumulative GDD class used for the prediction, i.e. 480–640 cumulative GDD class for tillering stage and 1120–1280 cumulative GDD class for ripening stage. Machine learning (ML) regression algorithms were used for rice yield prediction. Five ML algorithms were selected and compared: cubist (CUB, Quinlan, 1992), gaussian process regression (GPR, Williams, 1998), single-layer perceptron feedforward neural networks (NNET, Murtagh, 1991), random forest (RF, Breiman, 2001), and support vector regression with radial basis function kernels (SVM, Vapnik, 1998). The algorithms were implemented using the R package 'caret' (Kuhn, 2008).

2.4.2. Downscaling and upscaling approaches configuration

Downscaling and upscaling approaches were evaluated using two yield datasets: yield maps and whole-field-average yields. To obtain downscaling approach ML algorithms were trained with whole-field-average yields (238 data) and tested with yield maps (3674 data),

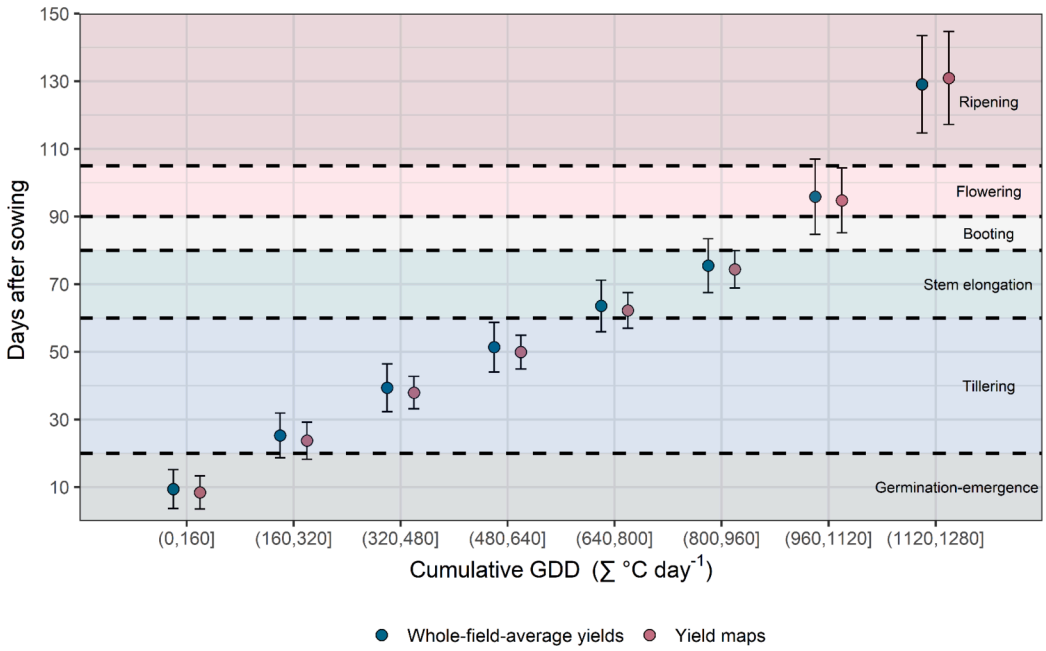


Fig. 3. Phenological stages of rice for each yield source data (i.e. whole-field-average yields and yield maps) grouped by cumulative GDD (∑ °C/day) and days after sowing.

while the opposite was done to obtain upscaling approach. In addition, to evaluate the effect of training and testing size on early season yield prediction two different set sizes were compared: the full set size (as mentioned previously) and the partial set size. The partial set size included the 238 data of whole-field-average yields and only 238 data of yield maps, which were selected based on the size and distribution of the whole-field-average yields data. These selected data were used as a testing set for the downscaling approach and as a training set for the upscaling approach. Hyper-parameters optimisation was obtained by a grid-searching method using a *k* fold cross-validation strategy with five folds in order to accurately evaluate the performance of each ML algorithm and to avoid the overfitting issues (Arlot and Celisse, 2010; Picard and Cook, 1984). A description of the hyper-parameters used for each ML algorithm is reported in Table S5.

2.4.3. Benchmark models configuration

Downscaling and upscaling approaches performances were compared with benchmark models, using data of whole-field-average yields for upscaling approach and of yield maps for downscaling approach. Two types of benchmark models were evaluated: null models and machine learning models. Null models are naive models where the yield prediction in this study was calculated as the average of measured data of whole-field-average yields and yield maps for evaluating upscaling and downscaling approaches, respectively. In addition, each ML algorithm was used as a benchmark model, splitting each whole-field-average yields and yield maps dataset into the training and testing set of the machine learning model. This procedure aimed to compare the performance of machine learning models trained and tested with a single yield source dataset, i.e. whole-field-average yields for the upscaling approach and yield maps for the downscaling approach. For the machine learning benchmark models, a nested leave-one-fold-out cross-validation strategy was adopted. This cross-validation strategy required splitting the data into an outer and inner cross-validation loop. In the outer cross-validation loop, the two datasets (i.e. whole-field-average yields and yield maps) were partitioned into non-overlapping folds and data from one-fold of the *n* available fold ($n = 5$) were held out. The remaining *n*-1 folds were used in an inner cross-validation loop. In the inner cross-validation loop, hyper-parameters optimisation was done using a *k-fold* cross-validation strategy with five folds. Following this approach, *n* different models were trained, one for each of the *n* outer loop folds, and all data were used for both calibration and validation.

2.5. Model evaluation

2.5.1. Performance metrics

Machine learning models were evaluated using four different performance metrics: the bias, the coefficient of determination (R^2), the normalised root mean square error (NRMSE), and the modelling efficiency (EF). Bias was calculated as the mean difference between measured and predicted values. Bias values close to 0 indicate that the model performs well. A positive bias indicates an under-prediction of the model, and a negative bias indicates an overprediction. R^2 values, ranging from 0 to 1, indicate the prediction performance of the models, with greater predictive accuracy at higher values. NRMSE was calculated using the average of the measured values to normalise the RMSE. Lower NRMSE values indicate high model performance, i.e. less difference between measured and predicted values. EF is a unitless measure that directly compares predictions with observed data (Pulina et al., 2022). An EF value of 0 means that the evaluated model achieved the same performance as a simple average of the measured data, while an EF value of 1 means a perfect match of measured and predicted values. If the EF value is less than 0, the predicted values are worse than simply using the measured average. In particular, for the ML benchmark models, the average of the performance metrics (bias, R^2, NRMSE, and EF) was calculated from the performance metrics obtained from each fold in the outer cross-validation loop (i.e. five folds).

2.5.2. Normalisation of performance metrics

Relative changes in models performances were analysed using a min–max normalisation procedure reported by Feng et al. (2020), to compare the downscaling and upscaling approaches with the corresponding ML benchmark models. Following this procedure, the R^2 and the NRMSE were normalised using the min–max values obtained at tillering and at ripening stages from the five ML algorithms of the benchmark models; they were referred to as nR^2 and nNRMSE, respectively.

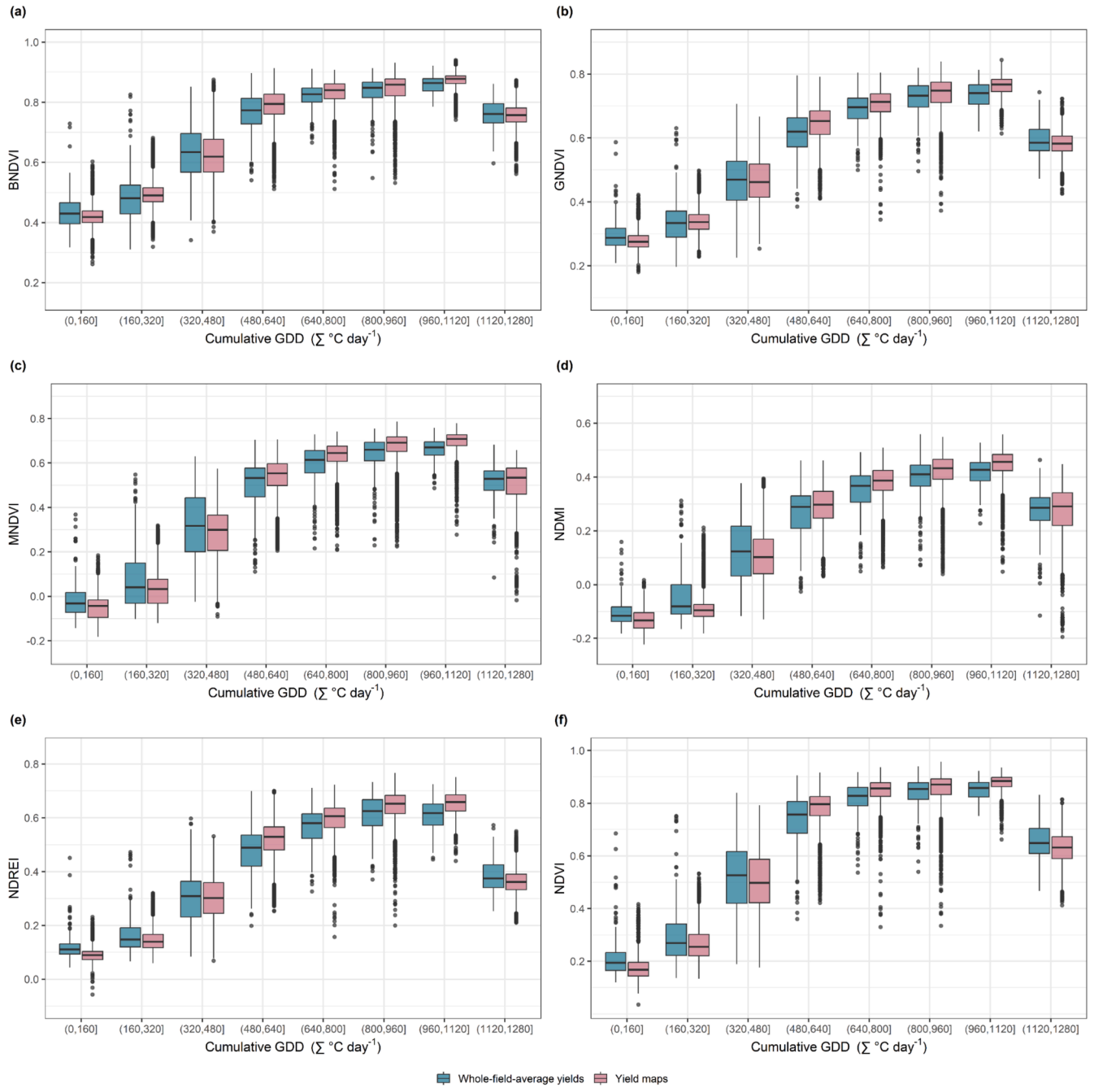


Fig. 4. Distribution of the average VIs of each phenological stage and yield source data (i.e. whole-field-average yields and yield maps). (a) BNDVI, (b) GNDVI, (c) MNDVI, (d) NDMI, (e) NDREI, and (f) NDVI.

2.5.3. Simple Additive Weighting method for Multi-Criteria decision analysis

To determine the suited ML algorithm for both downscaling and upscaling approaches for early season yield prediction applications, a Multi-Criteria Decision Analysis (MCDA) was performed using the Simple Additive Weighting (SAW) method (Churchman and Ackoff, 1954). The SAW method was used because of its simplicity. It is a multi-criteria procedure based on a weighted summation of rating the performance of each alternative on all alternative criteria. The best and recommended alternative is the one with the highest score. Four criteria were considered based on the performance metrics evaluated, i.e. the bias, the R^2, NRMSE, and EF, while the five ML algorithms were considered as alternatives. SAW requires a comparable scale for all elements in the decision matrix (Maimoun et al., 2016). The criteria, i.e. the performance metric values, were normalised from 0 to 1, representing the worst and best performance, respectively. The weight used in the SAW procedure was 0.25 (i.e. 1/4 where 4 is the number of criteria considered) and the same for each criterion.

3. Results

3.1. Performances of downscaling and upscaling approaches

The normalised R^2 (nR^2) and NRMSE (nNRMSE) values calculated by five machine learning (ML) algorithms (i.e. CUB, GPR, NNET, RF, and SVM) at two prediction times (i.e. tillering and ripening stages) are shown in Fig. 5 to compare the yield prediction accuracy between the downscaling and upscaling approaches with the corresponding ML

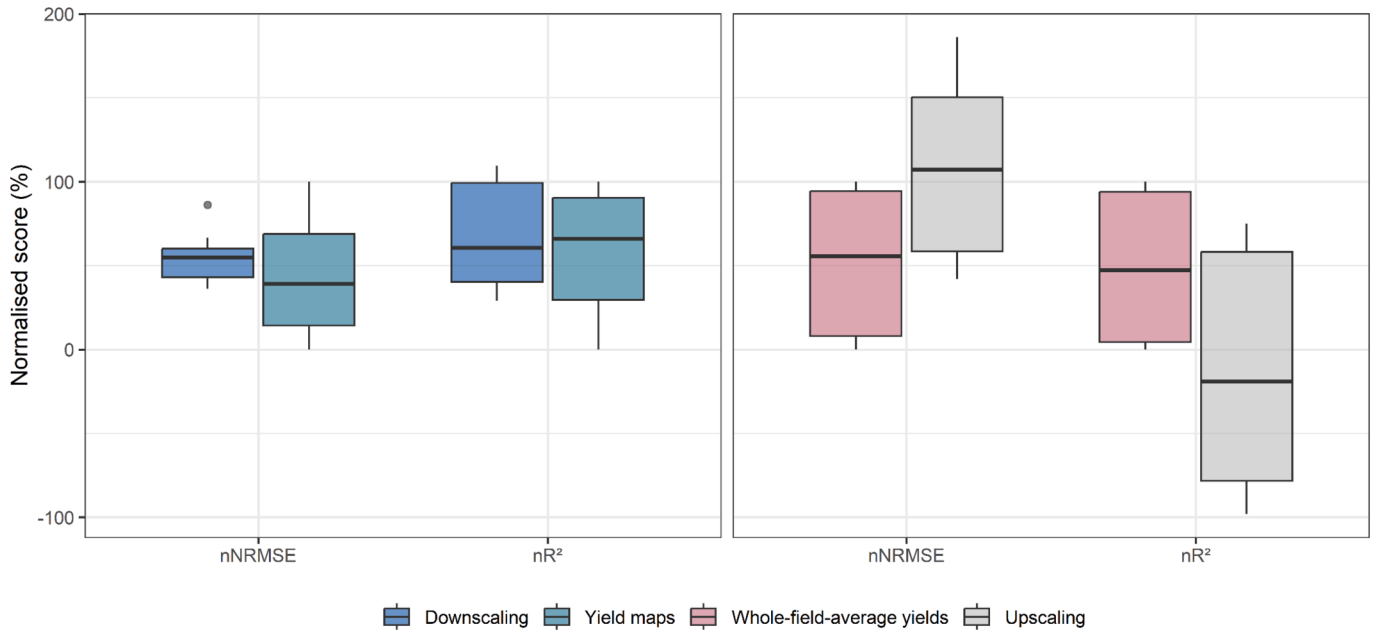


Fig. 5. Comparison of the downscaling and upscaling approaches performance by the distribution of the normalised values of NRMSE (nNRMSE) and R^2 (nR^2) obtained from five machine learning (ML) models (CUB, GPR, NNET, RF, and SVM) at the tillering and ripening stages. Yield maps and whole-field-average yields were considered ML benchmark models for downscaling and upscaling approaches, respectively.

benchmark models. Both the downscaling and upscaling approaches achieved lower accuracy compared to the related ML benchmark models (i.e. yield maps for the downscaling approach and whole-field-average yields for the upscaling approach, see Fig. 5); in fact, the downscaling and upscaling approaches showed the median of nR^2 lower than ML benchmark models and the median of nNRMSE higher than ML benchmark models (Fig. 5). In terms of approach comparison, the downscaling approach achieved similar accuracy to ML benchmark models (i.e. yield maps). In contrast, the accuracy of the upscaling approach showed a substantial decrease compared to ML benchmark models (i.e. whole-field-average yields).

3.2. Machine learning models prediction performances at tillering and ripening stages

The performance metrics of the ML models for the downscaling and upscaling approaches at the tillering and ripening stages are shown in Fig. 6 and in supplementary material Table S6. In general, the downscaling approach performed better than the upscaling approach, and for both approaches, the highest accuracy was achieved at the ripening stage compared to the tillering stage. The downscaling approach at tillering stage showed higher accuracy than upscaling in all ML models evaluated, and it showed less difference in accuracy between tillering and ripening stage than upscaling approach. For NRMSE (%), except for NNET at the tillering stage, all ML models performed better than the null model used as a benchmark model, represented by the dashed line and coloured according to the approaches (Fig. 6). For bias (Mg ha^{-1}), the null benchmark model generally performed better than the ML models; except for the RF and SVM downscaling approach at tillering stage, the CUB and SVM upscaling approach at tillering stage, and the GPR and RF upscaling approach at ripening stage. In general, at tillering stage, the highest prediction performance was achieved by the SVM model, for both downscaling and upscaling approaches. For the downscaling approach at the tillering stage, the SVM model achieved the highest accuracy for all the performance metrics, with 20 % of NRMSE, 0.56 of R^2, 0.53 of EF, and −0.01 of bias (Mg ha^{-1}), while the CUB model achieved the lowest accuracy for all the performance metrics, with 23.8 % of NRMSE, 0.49 of R^2, 0.33 of EF, and −0.62 of bias (Mg ha^{-1}). For the upscaling approach at the tillering stage, the SVM model achieved the highest accuracy for NRMSE, EF, and bias with 27.8 %, 0.22, and −0.04 (Mg ha^{-1}) respectively, while the NNET model achieved the lowest accuracy for NRMSE, R^2, and EF with 32.1 %, 0.12, and −0.05, respectively. The performance of the ML models at the tillering stage was as reliable as at the ripening stage, so further analysis shows only the ML performance at the tillering stage.

3.3. Validation of machine learning models for early season yield prediction

The validation of the machine learning (ML) models at the tillering stage for early yield prediction is shown in Fig. 7 both for the downscaling approach and for the upscaling approach. The figure showed the residuals (Mg ha^{-1}) of each ML model, and the distribution of the measured yield (i.e. the black line) and the predicted yield from each ML model. For the downscaling approach, when the measured yield was above 8 Mg ha^{-1}, the GPR, NNET and SVM models predicted the yield well. The CUB model overpredicted yield when the measured yield was above 10 Mg ha^{-1} and underpredicted yield when the measured yield was between 7 Mg ha^{-1} and 10 Mg ha^{-1}, while the opposite was obtained by the RF model. When the measured yield was below 5 Mg ha^{-1}, the ML models SVM and CUB predicted better than GPR, NNET and RF because they cannot predict the yield below 4 Mg ha^{-1}. For the upscaling approach, the ML models underpredicted yield when the measured yield was above 10 Mg ha^{-1} and below 6 Mg ha^{-1}, whereas they overpredicted yield when the measured yield was between 8 Mg ha^{-1} and 10 Mg ha^{-1}.

3.4. Effects of training and testing set size on early season yield prediction of machine learning models

The performance metrics of the ML models at the tillering stage both for both downscaling and upscaling approaches using the full set of measured yields (i.e. 238 whole-field-average yields data and 3674 yield maps data) were compared with the performances of ML models using only 238 data of yields (i.e. the full whole-field-average yields dataset and 238 data of yield maps selected based on the whole-field-average

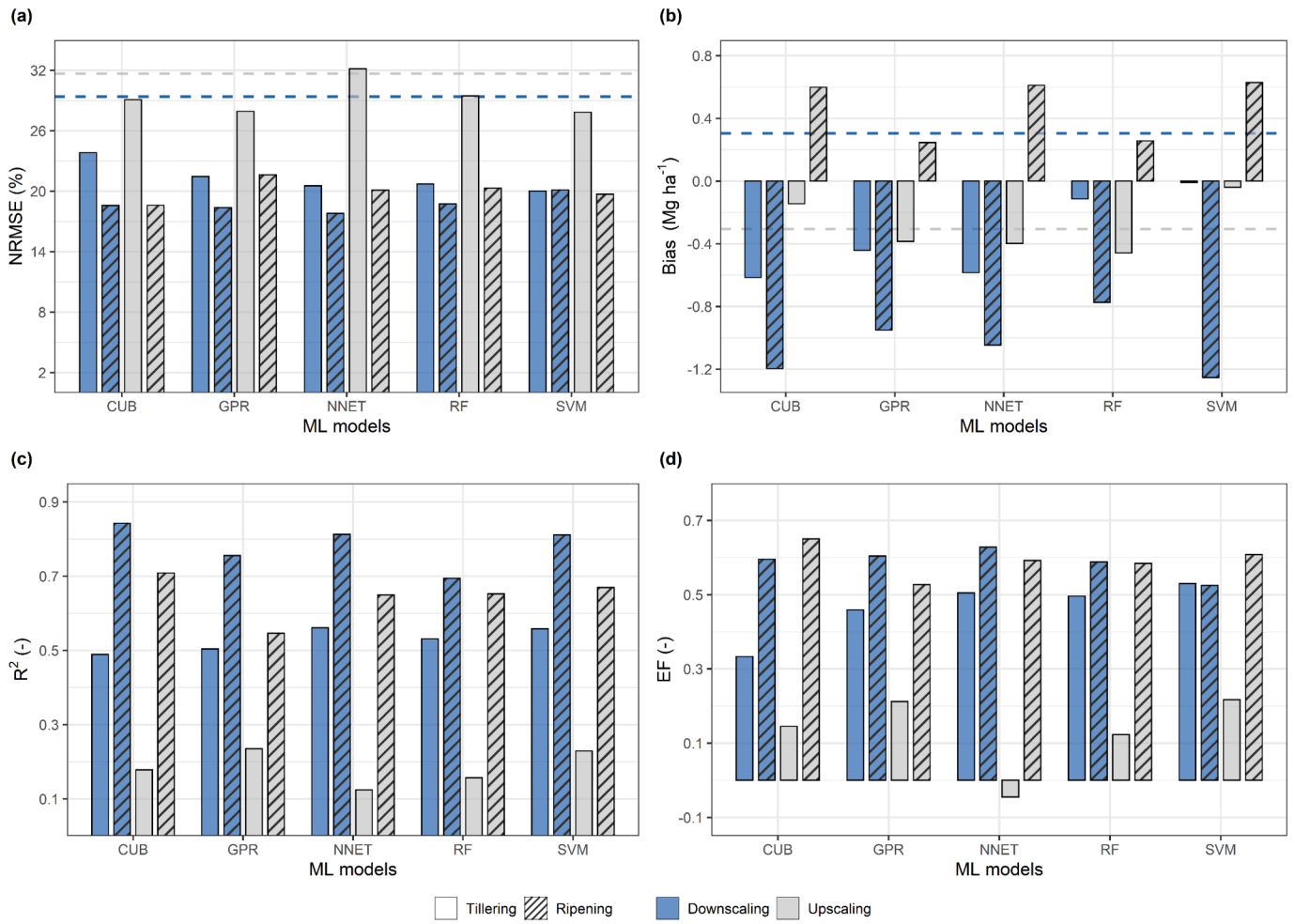


Fig. 6. Performance metrics of five machine learning (ML) models according to the different approaches (i.e. downscaling and upscaling) and phenological stages (i.e. tillering and ripening). The performance metrics evaluated were (a) NRMSE (%), (b) bias (Mg/ha), (c) R^2 (−), and (d) EF (−). The null models used as benchmark models are shown as dashed lines and coloured according to the approaches. The null models are the average of measured data of whole-field-average yields for the upscaling approach and of yield maps for the downscaling approach.

yields distribution). The results of this comparison are shown in Table 1. For the downscaling approach, a decrease in the performance of the ML models was observed when the testing set size was at 238 data, except for the EF values of the GPR and NNET models and for the R^2 values of the GPR, NNET, and RF models. For the upscaling approach, an increase in the performance of the ML models was observed when the training set size was at 238 data, except for the bias values of the CUB and SVM models.

To evaluate the effect of training and testing set size on the performance of ML models, the score of the Simple Additive Weighting (SAW) method are also reported in Table 1. The SAW score showed that the SVM model achieved the highest values with the full set size for both the downscaling and upscaling approaches, while the highest values with the 238 data set size for training and testing were achieved by NNET and RF for the downscaling approach and by GPR for the upscaling approach. For the downscaling approach, the SAW score decreased from 0.99 to 0.53 for SVM while it increased from 0.70 and 0.76 to 0.80 and 0.80 for NNET and RF, respectively. In particular, the SAW score of the RF showed a more stable in the set size comparison. For the upscaling approach, the SAW score decreased from 0.99 to 0.68 for SVM while it increased from 0.78 to 1.00 0 for GPR, which showed a more stable in the set size comparison.

3.5. *Early season yield prediction maps*

The two more stable ML algorithms, RF for the downscaling approach and GPR for the upscaling approach, were used to map the residuals of the ML models in the years 2020, 2021 and 2022. The RF residuals maps for the downscaling approach are shown in Fig. 8 and the GPR residuals maps for the upscaling approach are shown in Fig. 9. The ML models underpredicted the yield in 2020 and 2021, but the residuals were close to 0, for both the downscaling and upscaling approaches. The ML models overpredicted the yield in 2022 and the residuals were far from 0, for both downscaling and upscaling approaches.

4. Discussion

4.1. *Early season yield prediction for precision nitrogen fertilisation application*

A proactive approach to early season yield prediction is fundamental for the application of precision agriculture techniques such as site-specific nitrogen fertilisation. However, early rice yield prediction is a challenging and notoriously difficult task (Desloires et al., 2023). The proposed ML-based yield prediction at the tillering stage, using downscaling and upscaling approaches, could support rice farmers to precisely manage nitrogen use.

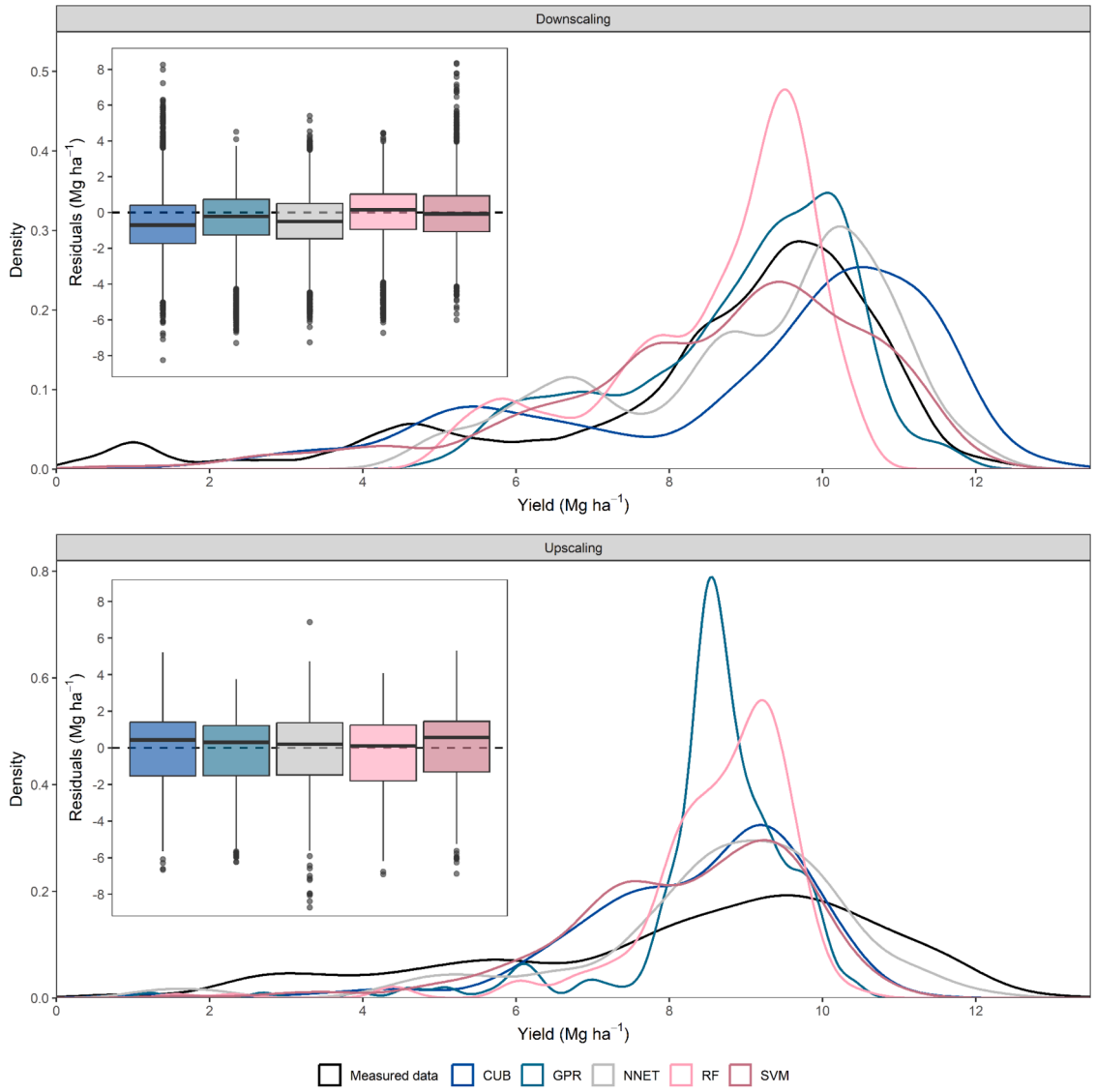


Fig. 7. Validation of the machine learning (ML) models at the tillering stage for both downscaling and upscaling approaches. Black lines represent the distribution of measured yield for the downscaling approach (i.e. yield maps) and the upscaling approach (whole-field-average yields). Coloured lines represent the predicted yield according to the ML models. The boxplots represent the residuals (Mg/ha) between the measured yield and the predicted yield according to the different ML models.

4.1.1. Tillering and ripening stages prediction times

In rice farming, predicting yield during the tillering stage is crucial for applying the correct amount of nitrogen fertilizer. This ensures a high yield and precision fertilization. In this study, rice yield prediction at tillering stage was compared with that at ripening stages. The performances of five machine learning (ML) models demonstrated that highest accuracy is obtained at the ripening stage than at the tillering stage. An increase in ML performance from vegetative growth stages to reproductive stages for yield prediction is reported in previous studies, such as Croci et al. (2022b) where the same ML algorithms evaluated in this study achieved the highest performance at the reproductive stage in maize. Similar results were obtained by Li et al. (2021) in rice, where the accuracy of the RF models increased from tillering, with an average of 0.71 of r (i.e. 0.50 of R^2), to ripening stages, with an average of 0.79 of r (i.e. 0.62 of R^2), for early, mid and late rice. The results obtained by Li et al. (2021) were similar to those obtained in this study, where the R^2 at tillering and ripening stages were 0.56 and 0.81, respectively, using the SVM algorithm. The rice phenological stages after the tillering stage are fundamental to determine the numbers of panicles that is one of the most important traits related to rice yield (Pasuquin et al., 2008). Several aspects, such as biotic and abiotic stresses, can reduce the accuracy of the ML models for early season yield prediction at vegetative growth stages (e.g. at the tillering stage). For example, in this study, the ML models cannot predict the biotic and abiotic stresses that may affect the rice crop after the tillering stage and thus affect rice yield (Iqbal et al., 2023). Among abiotic stresses, drought can reduce rice yield (Ijaz et al., 2019). In this study, the effect of a severe drought was observed in 2022, when rice yield was very low. In this case, the ML models overpredicted the yield at the tillering stage. This is probably either because drought conditions occurred after the tillering stage, or because poor data with low yield values were used to train the ML models. Previous studies (Cao et al., 2021a; Evans and Shen, 2021; Ruan et al., 2022) have suggested that the models can underpredict high yields and overpredict low yields. In general, the results obtained in this study highlighted that all ML models outperformed the null benchmark model (i.e. the mean yield that is generally used from rice farmers for nitrogen balance calculation) by a wide margin for both tillering and ripening stages. This highlights a great potential for ML models and supports their use for early season yield prediction. The ML models developed at the tillering stage demonstrated a reliable accuracy to determine low, medium, and high yield values. These values are relevant e.g. for precision nitrogen fertilisation, using management zones approach, or for the

Table 1
Performance metrics at the tillering stage of the machine learning (ML) models for the downscaling and upscaling approaches. Two different set size were compared, the full set size and the partial set size with 238 yield data for both training and testing set. The performance metrics were NRMSE (%), Bias (Mg/ha), R^2 (−), EF (−), and the SAW score (−). The SAW score was calculated using Simple Additive Weighting (SAW) method. It is a multi-criteria procedure based on the concept of a weighted summation of rating the performance of each alternative (i.e. CUB, GPR, NNET, RF, and SVM models) on all alternative criteria (i.e. NRMSE, Bias, R^2, and EF). The best and recommended alternative is the one with the highest score. The highest performance for each metric were highlighted in bold.

Approach	Metric	Set size (train:test)	CUB	GPR	NNET	RF	SVM
Downscaling	**NRMSE (%)**	238:3674	23.8	21.5	20.5	20.7	**20.0**
		238:238	26.3	22.5	**21.8**	22.4	23.8
	Bias (Mg/ha)	238:3674	−0.62	−0.44	−0.58	−0.11	**−0.01**
		238:238	−0.75	−0.57	−0.62	−0.30	**−0.15**
	R^2 (−)	238:3674	0.49	0.50	**0.56**	0.53	**0.56**
		238:238	0.47	0.57	**0.59**	0.55	0.47
	EF (−)	238:3674	0.33	0.46	0.51	0.50	**0.53**
		238:238	0.31	0.50	**0.53**	0.50	0.44
	SAW score (−)	238:3674	0.00	0.44	0.70	0.76	**0.99**
		238:238	0.01	0.71	**0.80**	**0.80**	0.53
Upscaling	**NRMSE (%)**	3674:238	29.1	27.9	32.1	29.4	**27.8**
		238:238	27.8	**27.0**	27.8	28.4	27.4
	Bias (Mg/ha)	3674:238	−0.15	−0.39	−0.40	−0.46	**−0.04**
		238:238	−0.28	**−0.17**	0.25	−0.35	0.20
	R^2 (−)	3674:238	0.18	**0.24**	0.12	0.16	0.23
		238:238	0.23	**0.29**	0.26	0.21	0.25
	EF (−)	3674:238	0.15	0.21	−0.05	0.12	**0.22**
		238:238	0.22	**0.26**	0.22	0.18	0.24
	SAW score (−)	3674:238	0.67	0.78	0.04	0.39	**0.99**
		238:238	0.37	**1.00**	0.52	0.00	0.68

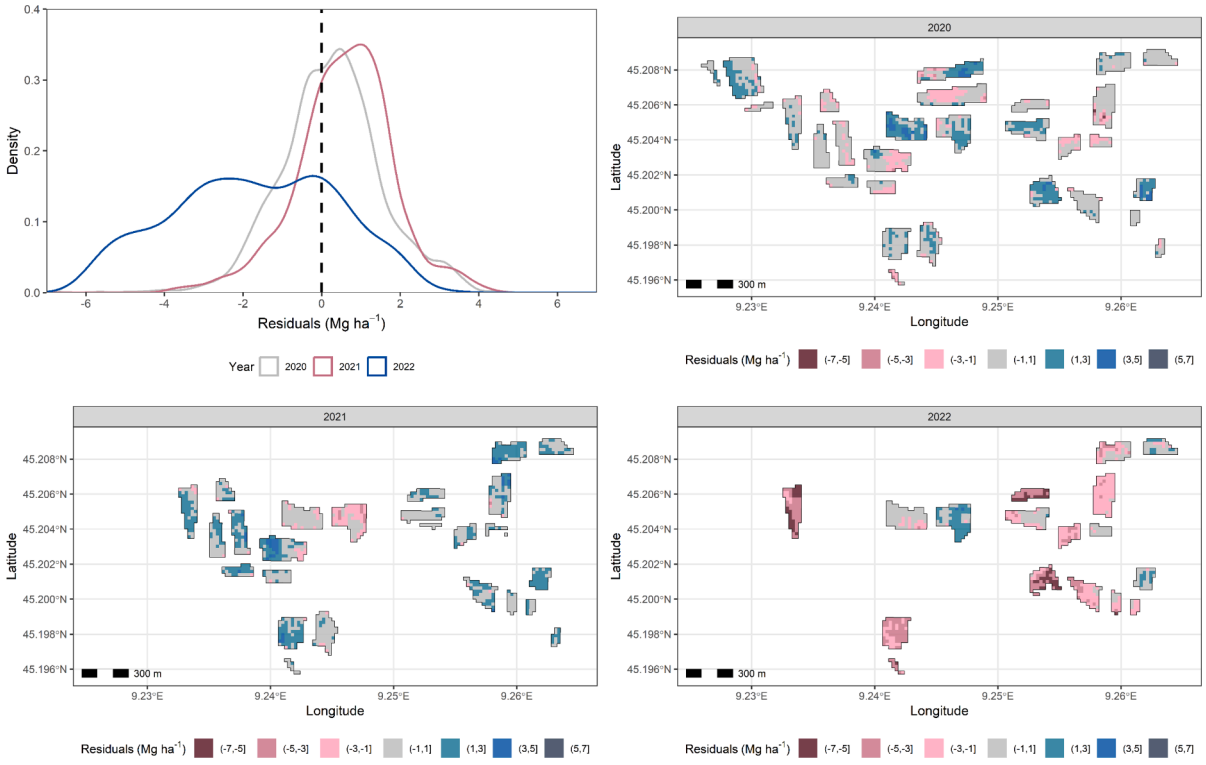


Fig. 8. Distribution and maps of the RF model residuals of the downscaling approach during the years 2020, 2021, and 2022.

determination of the spatio-temporal variability and stability of crop yield over years. These ML models can prevent overfertilisation and minimise nitrogen loss in both low and high yielding fields, as suggested by Ruan et al. (2022). Despite the promising results of this study to improve precision nitrogen fertilisation, the wider adoption of these techniques remains limited by several barriers, including high costs, limited knowledge and the prevalence of small farm sizes (Blasch et al., 2022; Masi et al., 2023). Although precision agriculture offers significant benefits, its uptake across Europe has been limited (Kutter et al., 2011; Reichardt et al., 2009). One of the main barriers is the significant initial investment required for variable rate technology (VRT), which often discourages small- and medium-sized farmers, as the potential economic returns may not justify the upfront costs, especially for smaller plots. The problem is further exacerbated by a lack of technical knowledge and training on how to effectively implement and maximise the value of these technologies (Vecchio et al., 2022). In addition, the small size of farms and the incompatibility of existing machinery with VRT pose significant technical challenges, making it difficult to integrate these advanced technologies (Kutter et al., 2011; Reichardt et al., 2009).

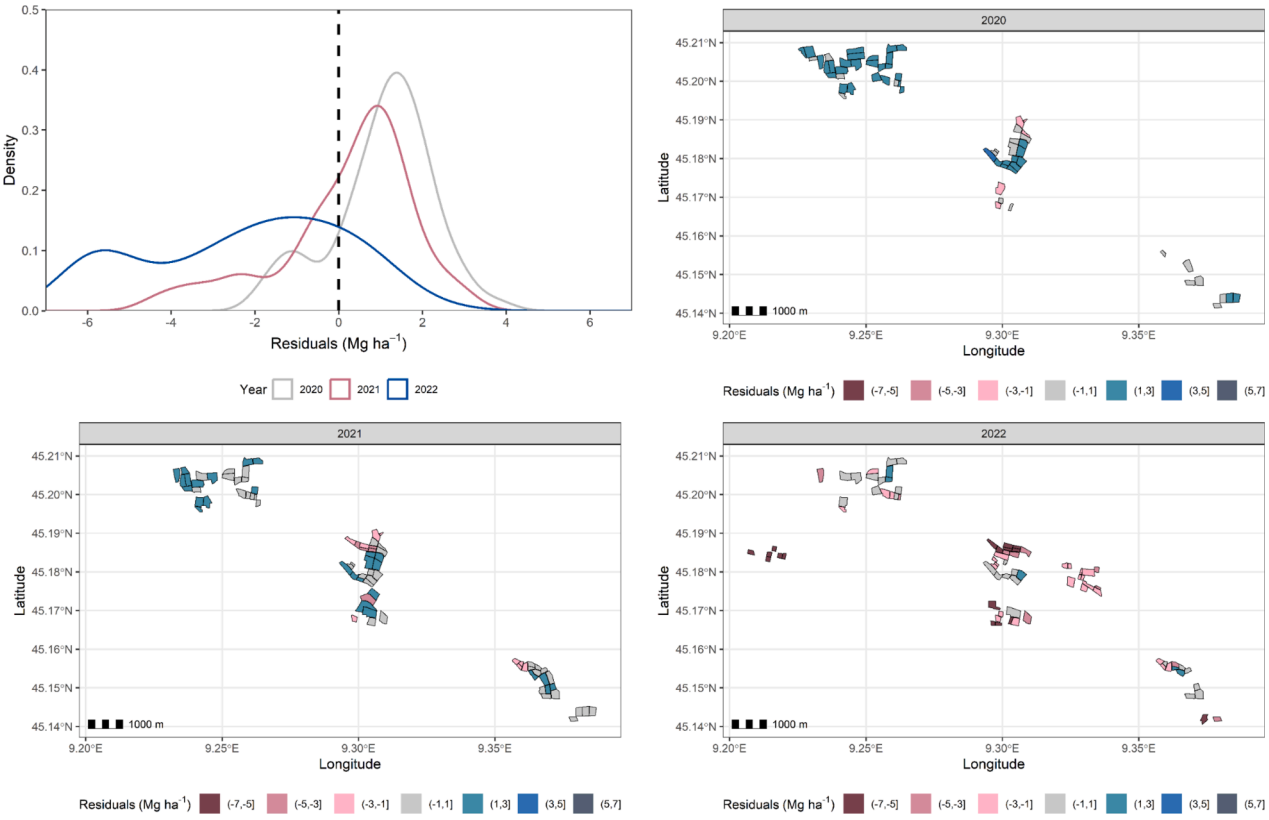


Fig. 9. Distribution and maps of the GPR model residuals of the upscaling approach during the years 2020, 2021, and 2022.

4.1.2. *Downscaling and upscaling approaches comparison*

Higher performances were obtained by downscaling approach than upscaling approach. The downscaling approach achieved similar performance of the ML benchmark models that were trained and tested with yield maps dataset. This is important because the ML benchmark models can be affected by spatial autocorrelation, which can inflate performance metrics and limit their transferability to new data (Kattenborn et al., 2022). These results suggest that the downscaling approach could support precision nitrogen fertilisation in rice both for a site-specific nitrogen fertilisation and for the delineation of management zones by identifying yield stability zones using multi-year data. The performance metrics obtained using the downscaling approach were lower compared to the NRMSE reported by Gilardelli et al. (2019) in a downscaled rice yield simulation. However, it is difficult to compare these studies because two different downscaling approaches were used. In this study, ML models were used, while in Gilardelli et al. (2019), the satellite retrieved leaf area index was assimilated into a rice growth model. Comparing the performance metrics of ML models with other studies that performed an early season prediction, similar results of R^2 were reported by Meroni et al. (2021) for wheat, by Desloires et al. (2023) for maize, and by Yang et al. (2022) for rice while higher results were reported by Son et al. (2022), Cao et al. (2021b), Lingwal et al. (2022) for rice. The comparison of model accuracy across studies remains a daunting task, largely due to the reliance on performance metrics like RMSE and NRMSE, which are strongly influenced by the characteristics of the validation data (Impollonia et al., 2022a). Furthermore, Schauberger et al. (2020) emphasize the absence of validation through independent test sets in the majority of ML studies.

4.1.3. *Effects of set sizes on machine learning performances*

The characteristics of the training and testing sets, such as size (Millard and Richardson, 2015) and range of values (Shah et al., 2019), are also relevant features to evaluate the performance of ML models, as reported by Impollonia et al. (2022b). Kamir et al. (2020) reported that ML models were sensitive to an increase in the size of the training set, while Johnson (2016) reported that additional training data from years with high or low yields improved the accuracy of the yield prediction. For these reasons, in this study, to accurately evaluate and compare the different ML models for early season rice yield prediction for both downscaling and upscaling approaches, ML algorithms were trained and tested with different set sizes. The results highlighted the importance of training and testing set sizes on the performance of ML models. Considering the full set size, the SVM model achieved the highest performance for both downscaling and upscaling approaches, showing high transferability between the two different yield data sources used in this study (whole-field-average yields and yield maps). However, when the ML algorithms were trained and tested with only 238 yield data following the distribution of whole-field-average yields, the performance metrics of the SVM models, like the Simple Additive Weighting (SAW) score, decreased enough. On the contrary, the RF and GPR algorithms showed a more transferable and stable in the set size comparison and they therefore were used for the early season rice yield prediction for the application of precision nitrogen fertilisation.

4.2. *Advantages, limitations and perspectives*

A relevant novelty of this study was the evaluation of the downscaling and upscaling approaches using ML models for field-scale rice yield prediction at the tillering stage for precision nitrogen fertilisation. Transferable ML models were developed using the spatio-temporal variations of the two sources of yield data (i.e. yield maps and whole-field average yields) provided by multi-genotype, multi-site, and multi-year on rice fields. The different set sizes of the whole-field average yields and yield maps are intrinsic features of the two yield data sources in which whole-field average yields are considered poor data while yield maps are considered rich data. The result of the ML

performance highlighted the interesting use of the downscaling approach to reduce the number of training data required for an accurate yield prediction. In addition, this approach could substitute the yield maps where they cannot be collected due to lack of yield harvesting machinery. The use of thermal time to estimate rice phenology increased the transferability and scalability of ML models. Several studies reported an increase in the performance of models using thermal time compared to calendar time (Desloires et al., 2023; Durgun et al., 2020). Desloires et al. (2023) suggested that the advantage of using thermal time is due to a more consistent representation of crop physiology, which reduces domain mismatch between training and testing years. From a machine learning perspective, the results could also be improved by using deep learning techniques; indeed, several studies have reported promising accuracy (Cao et al., 2021a, 2021b; Liu et al., 2022). However, Sabo et al. (2023) reported that ML models outperformed deep learning models for wheat yield prediction. The authors attributed the small size of the available dataset to the poor performance of deep learning models. A limitation of this study is the data-poor context of the downscaling approach, which considered a small set size (i.e. 238 whole-field average yield data) with only five years of yield data. As a result, future studies should increase the set size to improve the reliability and transferability of the results, as also suggested by Zhang et al. (2023), and the use of a large set size could also enable the correct evaluation of deep learning techniques. Another limitation of this study is the small geographical area considered, in fact rice yield data were only collected in one province of Northern Italy. This limitation is relevant because the ML models developed could suffer from limited transferability to other geographical areas, thus limiting their large-scale application. The high spatial resolution of the Sentinel-2 derived vegetation indices (VIs) enabled to acquire of within-field yield variability in this study. However, VIs are limited in capturing the full yield variability because they ignore physiological yield mechanisms. In fact, yield is determined by several factors such as genotype, soil characteristics, agronomic management and weather data (Sihi et al., 2022). Several studies have highlighted the great potential of adding weather (Croci et al., 2022b; Yu et al., 2023) and soil data (Li et al., 2021; Rigden et al., 2020) for yield prediction, and future studies could focus on incorporating this into ML models. The use of weather data could improve the transferability of ML models between years, particularly in years with low or high yields, as observed in this study for the 2022 growing season, which was particularly affected by drought conditions. On the other hand, using many predictors could lead to overfitting and dimensionality problems, especially if the number of predictors is larger than the size of the training set (Subramanian and Simon, 2013). In addition, in order to take advantage of the increased transferability of weather data, it is necessary to have a large dataset covering many years, especially due to climate change scenarios. For these reasons, in many cases, only the use of VIs could improve the transferability of ML models, as they could also be applied to years with extreme weather events.

5. Conclusion

This study proposed a machine learning (ML) model-based approach for early season rice yield prediction, at the tillering stage, to support precision nitrogen fertilisation. A novel aspect of this study was the use of ML models for rice yield prediction at the field scale, both through upscaling and downscaling approaches. The ML models outperformed the null benchmark model and similar performance was obtained between the downscaling approach and the ML benchmark models. The downscaling approach was more accurate than the upscaling approach and it could support rice farmers in applying site-specific nitrogen fertilisation based on within-field variability in yield prediction. This approach could support rice farmers to accurately manage nitrogen use through the adoption of precision agriculture techniques. Although this study provides valuable insights, it has some limitations, such as the small set size of the downscaling approach and the small geographical area considered, which may affect the early season yield prediction of machine learning models for large-scale applications.

CRediT authorship contribution statement

Giorgio Impollonia: Writing – original draft, Visualization, Software, Methodology, Investigation, Formal analysis, Data curation, Conceptualization. **Michele Croci:** Writing – review & editing, Methodology, Conceptualization. **Stefano Amaducci:** Writing – review & editing.

Declaration of competing interest

The authors declare that they have no known competing financial interests or personal relationships that could have appeared to influence the work reported in this paper.

Acknowledgements

Michele Croci was partially supported by 'National Research Centre for Agricultural Technologies (Agritech)' CN00000022. PNRR-M4C2, Investment 1.4 - Funded by the European Union - NextGenerationEU' - CUP: J33C22001160007.

Data statement.

The data that support the findings of this work are available from the corresponding author upon reasonable request.

Appendix A. Supplementary data

Supplementary data to this article can be found online at https://doi.org/10.1016/j.compag.2024.109603.

Data availability

Data will be made available on request.

References

Adhikari, K., Smith, D.R., Hajda, C., Kharel, T.P., 2023. Within-field yield stability and gross margin variations across corn fields and implications for precision conservation. Precis. Agric. 24, 1401–1416. https://doi.org/10.1007/s11119-023-09995-7.

Ali, A.M., Abouelghar, M., Belal, A.A., Saleh, N., Yones, M., Selim, A.I., Amin, M.E.S., Elwesemy, A., Kucher, D.E., Maginan, S., Savin, I., 2022. Crop yield prediction using multi sensors remote sensing (review article). Egypt. J. Remote Sens. Space Sci. 25, 711–716. https://doi.org/10.1016/j.ejrs.2022.04.006.

Arcieri, M., Ghinassi, G., 2020. Rice cultivation in Italy under the threat of climatic change: Trends, technologies and research gaps. Irrig. Drain. 69, 517–530. https://doi.org/10.1002/IRD.2472.

Arlot, S., Celisse, A., 2010. A survey of cross-validation procedures for model selection. Stat. Surv. 4. https://doi.org/10.1214/09-SS054.

Asseng, S., Ewert, F., Rosenzweig, C., Jones, J.W., Hatfield, J.L., Ruane, A.C., Boote, K.J., Thorburn, P.J., Rötter, R.P., Cammarano, D., Brisson, N., Basso, B., Martre, P., Aggarwal, P.K., Angulo, C., Bertuzzi, P., Biernath, C., Challinor, A.J., Doltra, J., Gayler, S., Goldberg, R., Grant, R., Heng, L., Hooker, J., Hunt, L.A., Ingwersen, J., Izaurralde, R.C., Kersebaum, K.C., Müller, C., Naresh Kumar, S., Nendel, C., O'Leary, G., Olesen, J.E., Osborne, T.M., Palosuo, T., Priesack, E., Ripoche, D., Semenov, M.A., Shcherbak, I., Steduto, P., Stöckle, C., Stratonovitch, P., Streck, T., Supit, I., Tao, F., Travasso, M., Waha, K., Wallach, D., White, J.W., Williams, J.R., Wolf, J., 2013. Uncertainty in simulating wheat yields under climate change. Nature Climate Change 3 (9), 827–832. https://doi.org/10.1038/nclimate1916.

Bacenetti, J., Paleari, L., Tartarini, S., Vesely, F.M., Foi, M., Movedi, E., Ravasi, R.A., Bellopede, V., Durello, S., Ceravolo, C., Amicizia, F., Confalonieri, R., 2020. May smart technologies reduce the environmental impact of nitrogen fertilization? A case study for paddy rice. Sci. Total Environ. 715, 136956. https://doi.org/10.1016/j.scitotenv.2020.136956.

Basso, B., Liu, L., 2019. Seasonal crop yield forecast: Methods, applications, and accuracies. Advances in Agronomy 154, 201–255. https://doi.org/10.1016/bs.agron.2018.11.002.

Bassu, S., Fumagalli, D., Toreti, A., Ceglar, A., Giunta, F., Motzo, R., Zajac, Z., Niemeyer, S., 2021. Modelling potential maize yield with climate and crop conditions around flowering. Field Crops Res 271, 108226. https://doi.org/10.1016/J.FCR.2021.108226.

Blasch, J., van der Kroon, B., van Beukering, P., Munster, R., Fabiani, S., Nino, P., Vanino, S., 2022. Farmer preferences for adopting precision farming technologies: a case study from Italy. Eur. Rev. Agric. Econ. 49, 33–81. https://doi.org/10.1093/erae/jbaa031.

Bouma, J., 2007. Precision agriculture: introduction to the spatial and temporal variability of environmental quality. In: Ciba Foundation Symposium 210-Precision Agriculture: Spatial and Temporal Variability of Environmental Quality: Precision Agriculture: Spatial and Temporal Variability of Environmental Quality: Ciba Foundation Symposium 210. John Wiley & Sons, Ltd, Chichester, UK, pp. 5–17. https://doi.org/10.1002/9780470515419.ch2.

Breiman, L., 2001. Random forests. Mach. Learn. 45, 5–32. https://doi.org/10.1023/A:1010933404324.

Busetto, L., Casteleyn, S., Granell, C., Pepe, M., Barbieri, M., Campos-Taberner, M., Casa, R., Collivignarelli, F., Confalonieri, R., Crema, A., Garcia-Haro, F.J., Gatti, L., Gitas, I.Z., Gonzalez-Perez, A., Grau-Muedra, G., Guarneri, T., Holecz, F., Katsantonis, D., Minakou, C., Miralles, I., Movedi, E., Nutini, F., Pagani, V., Palombo, A., Paola, F.D., Pascucci, S., Pignatti, S., Rampini, A., Ranghetti, L., Ricciardelli, E., Romano, F., Stavrakoudis, D.G., Stroppiana, D., Viggiano, M., Boschetti, M., 2017. Downstream Services for rice crop monitoring in Europe: from regional to local scale. IEEE J. Sel. Top. Appl. Earth Obs. Remote Sens. 10, 5423–5441. https://doi.org/10.1109/JSTARS.2017.2679159.

Caloiero, T., Caroletti, G.N., Coscarelli, R., 2021. IMERG-based meteorological drought analysis over italy. Climate 9, 65. https://doi.org/10.3390/cli9040065.

Cammarano, D., Ceccarelli, S., Grando, S., Romagosa, I., Benbelkacem, A., Akar, T., Al-Yassin, A., Pecchioni, N., Francia, E., Ronga, D., 2019. The impact of climate change on barley yield in the Mediterranean basin. Eur. J. Agron. 106, 1–11. https://doi.org/10.1016/J.EJA.2019.03.002.

Cammarano, D., Liu, B., Liu, L., Ruane, A.C., Zhu, Y., 2021. Potential impacts of projected warming scenarios on winter wheat in the UK. J. Agric. Sci. 159, 511–522. https://doi.org/10.1017/S0021859621000903.

Cao, J., Zhang, Z., Luo, Y., Zhang, L., Zhang, J., Li, Z., Tao, F., 2021a. Wheat yield predictions at a county and field scale with deep learning, machine learning, and google earth engine. Eur. J. Agron. 123, 126204. https://doi.org/10.1016/j.eja.2020.126204.

Cao, J., Zhang, Z., Tao, F., Zhang, L., Luo, Y., Zhang, J., Han, J., Xie, J., 2021b. Integrating multi-source data for rice yield prediction across china using machine learning and deep learning approaches. Agric. For. Meteorol. 297, 108275. https://doi.org/10.1016/j.agrformet.2020.108275.

Choudhary, K., Shi, W., Dong, Y., Paringer, R., 2022. Random forest for rice yield mapping and prediction using sentinel-2 data with google earth engine. Adv. Space Res. 70, 2443–2457. https://doi.org/10.1016/j.asr.2022.06.073.

Churchman, C.W., Ackoff, R.L., 1954. An approximate measure of value. J. Oper. Res. Soc. Am. 2, 172–187. https://doi.org/10.1287/opre.2.2.172.

Coldiretti, 2022. Clima: al via la raccolta di riso italiano, -30% produzione [WWW Document]. https://www.coldiretti.it/economia/clima-al-via-la-raccolta-di-riso-italiano-30-produzione.

Croci, M., Impollonia, G., Marcone, A., Antonucci, G., Letterio, T., Colauzzi, M., Vignudelli, M., Ventura, F., Anconelli, S., Amaducci, S., 2022a. RTM inversion through predictive equations for multi-crop LAI retrieval using sentinel-2 images. Agronomy 12, 2835. https://doi.org/10.3390/AGRONOMY12112835/S1.

Croci, M., Impollonia, G., Meroni, M., Amaducci, S., 2022b. Dynamic maize yield predictions using machine learning on multi-source data. Remote Sens (Basel) 15, 100. https://doi.org/10.3390/rs15010100.

Demirhan, H., Renwick, Z., 2018. Missing value imputation for short to mid-term horizontal solar irradiance data. Appl. Energy 225, 998–1012. https://doi.org/10.1016/j.apenergy.2018.05.054.

Desloires, J., Ienco, D., Botrel, A., 2023. Out-of-year corn yield prediction at field-scale using Sentinel-2 satellite imagery and machine learning methods. Comput. Electron. Agric. 209, 107807. https://doi.org/10.1016/j.compag.2023.107807.

Duque, A.F., Patino, D., Colorado, J.D., Petro, E., Rebolledo, M.C., Mondragon, I.F., Espinosa, N., Amezquita, N., Puentes, O.D., Mendez, D., Jaramillo-Botero, A., 2023. Characterization of rice yield based on biomass and SPAD-based leaf nitrogen for large genotype plots. Sensors 23, 5917. https://doi.org/10.3390/s23135917.

Durgun, Y.Ö., Gobin, A., Duveiller, G., Tychon, B., 2020. A study on trade-offs between spatial resolution and temporal sampling density for wheat yield estimation using both thermal and calendar time. Int. J. Appl. Earth Obs. Geoinf. 86, 101988. https://doi.org/10.1016/j.jag.2019.101988.

Evans, F.H., Shen, J., 2021. Long-term hindcasts of wheat yield in fields using remotely sensed phenology, climate data and machine learning. Remote Sens (Basel) 13, 2435. https://doi.org/10.3390/rs13132435.

Feng, P., Wang, B., Liu, D.L., Waters, C., Xiao, D., Shi, L., Yu, Q., 2020. Dynamic wheat yield forecasts are improved by a hybrid approach using a biophysical model and machine learning technique. Agric. For. Meteorol. 285–286, 107922. https://doi.org/10.1016/j.agrformet.2020.107922.

Gerten, D., Heck, V., Jägermeyr, J., Bodirsky, B.L., Fetzer, I., Jalava, M., Kummu, M., Lucht, W., Rockström, J., Schaphoff, S., Schellnhuber, H.J., 2020. Feeding ten billion people is possible within four terrestrial planetary boundaries. Nature Sustainability 3 (3), 200–208. https://doi.org/10.1038/s41893-019-0465-1.

Gilardelli, C., Stella, T., Confalonieri, R., Ranghetti, L., Campos-Taberner, M., García-Haro, F.J., Boschetti, M., 2019. Downscaling rice yield simulation at sub-field scale using remotely sensed LAI data. Eur. J. Agron. 103, 108–116. https://doi.org/10.1016/J.EJA.2018.12.003.

Gitelson, A.A., Kaufman, Y.J., Merzlyak, M.N., 1996. Use of a green channel in remote sensing of global vegetation from EOS-MODIS. Remote Sens. Environ. 58, 289–298. https://doi.org/10.1016/S0034-4257(96)00072-7.

Gitelson, A., Merzlyak, M.N., 1994. Quantitative estimation of chlorophyll-a using reflectance spectra: experiments with autumn chestnut and maple leaves. J. Photochem. Photobiol. B 22, 247–252. https://doi.org/10.1016/1011-1344(93)06963-4.

Gorelick, N., Hancher, M., Dixon, M., Ilyushchenko, S., Thau, D., Moore, R., 2017. Google earth engine: planetary-scale geospatial analysis for everyone. Remote Sens. Environ. 202, 18–27. https://doi.org/10.1016/j.rse.2017.06.031.

Granell, C., Miralles, I., Rodríguez-Pupo, L.E., González-Pérez, A., Casteleyn, S., Busetto, L., Pepe, M., Boschetti, M., Huerta, J., 2017. Conceptual Architecture and Service-Oriented Implementation of a Regional Geoportal for Rice Monitoring. ISPRS International Journal of Geo-Information 6, 191. https://doi.org/10.3390/IJGI6070191.

Guarin, J.R., Martre, P., Ewert, F., Webber, H., Dueri, S., Calderini, D., Reynolds, M., Molero, G., Miralles, D., Garcia, G., Slafer, G., Giunta, F., Pequeno, D.N.L., Stella, T., Ahmed, M., Alderman, P.D., Basso, B., Berger, A.G., Bindi, M., Bracho-Mujica, G., Cammarano, D., Chen, Y., Dumont, B., Rezaei, E.E., Fereres, E., Ferrise, R., Gaiser, T., Gao, Y., Garcia-Vila, M., Gayler, S., Hochman, Z., Hoogenboom, G., Hunt, L.A., Kersebaum, K.C., Nendel, C., Olesen, J.E., Palosuo, T., Priesack, E., Pullens, J.W.M., Rodríguez, A., Rötter, R.P., Ramos, M.R., Semenov, M.A., Senapati, N., Siebert, S., Srivastava, A.K., Stöckle, C., Supit, I., Tao, F., Thorburn, P., Wang, E., Weber, T.K.D., Xiao, L., Zhang, Z., Zhao, C., Zhao, J., Zhao, Z., Zhu, Y., Asseng, S., 2022. Evidence for increasing global wheat yield potential. Environ. Res. Lett. 17, 124045. https://doi.org/10.1088/1748-9326/ACA77C.

Hasegawa, T., Wakatsuki, H., Ju, H., Vyas, S., Nelson, G.C., Farrell, A., Deryng, D., Meza, F., Makowski, D., 2022. A global dataset for the projected impacts of climate change on four major crops. Scientific Data 9 (1), 58. https://doi.org/10.1038/s41597-022-01150-7.

Ijaz, M., Qamar, S., Bukhari, S.A., Malik, K., 2019. Abiotic stress signaling in rice crop. In: Advances in rice research for abiotic stress tolerance. Woodhead Publishing, pp. 551–569. https://doi.org/10.1016/B978-0-12-814332-2.00027-7.

Impollonia, G., Croci, M., Blandinières, H., Marcone, A., Amaducci, S., 2022a. Comparison of PROSAIL model inversion methods for estimating leaf chlorophyll content and LAI using UAV imagery for hemp phenotyping. Remote Sens (Basel) 14, 5801. https://doi.org/10.3390/rs14225801.

Impollonia, G., Croci, M., Martani, E., Ferrarini, A., Kam, J., Trindade, L.M., Clifton-Brown, J., Amaducci, S., 2022b. Moisture content estimation and senescence phenotyping of novel Miscanthus hybrids combining UAV-based remote sensing and machine learning. GCB Bioenergy 14, 639–656. https://doi.org/10.1111/gcbb.12930.

Iqbal, J., Yousaf, U., Asgher, A., Dilshad, R., Qamar, F.M., Bibi, S., Rehman, S.U., Haroon, M., 2023. Sustainable Rice Production Under Biotic and Abiotic Stress Challenges. In: Sustainable Agriculture in the Era of the OMICs Revolution. Springer International Publishing, Cham, pp. 241–268. https://doi.org/10.1007/978-3-031-15568-0_11.

Jägermeyr, J., Müller, C., Ruane, A.C., Elliott, J., Balkovic, J., Castillo, O., Faye, B., Foster, I., Folberth, C., Franke, J.A., Fuchs, K., Guarin, J.R., Heinke, J., Hoogenboom, G., Iizumi, T., Jain, A.K., Kelly, D., Khabarov, N., Lange, S., Lin, T.S., Liu, W., Mialyk, O., Minoli, S., Moyer, E.J., Okada, M., Phillips, M., Porter, C., Rabin, S.S., Scheer, C., Schneider, J.M., Schyns, J.F., Skalsky, R., Smerald, A., Stella, T., Stephens, H., Webber, H., Zabel, F., Rosenzweig, C., 2021. Climate impacts on global agriculture emerge earlier in new generation of climate and crop models. Nature Food 2 (11), 873–885. https://doi.org/10.1038/s43016-021-00400-y.

Jeong, S., Ko, J., Yeom, J.M., 2022. Predicting rice yield at pixel scale through synthetic use of crop and deep learning models with satellite data in South and North Korea. Sci. Total Environ. 802, 149726. https://doi.org/10.1016/J.SCITOTENV.2021.149726.

Johnson, D.M., 2016. A comprehensive assessment of the correlations between field crop yields and commonly used MODIS products. Int. J. Appl. Earth Obs. Geoinf. 52, 65–81. https://doi.org/10.1016/j.jag.2016.05.010.

Jurgens, C., 1997. The modified normalized difference vegetation index (mNDVI) a new index to determine frost damages in agriculture based on Landsat TM data. Int. J. Remote Sens. 18, 3583–3594. https://doi.org/10.1080/014311697216810.

Kamir, E., Waldner, F., Hochman, Z., 2020. Estimating wheat yields in Australia using climate records, satellite image time series and machine learning methods. ISPRS J. Photogramm. Remote Sens. 160, 124–135. https://doi.org/10.1016/j.isprsjprs.2019.11.008.

Kasampalis, D.A., Alexandridis, T.K., Deva, C., Challinor, A., Moshou, D., Zalidis, G., 2018. Contribution of Remote Sensing on Crop Models: A Review. Journal of Imaging 4, 52. https://doi.org/10.3390/JIMAGING4040052.

Kattenborn, T., Schiefer, F., Frey, J., Feilhauer, H., Mahecha, M.D., Dormann, C.F., 2022. Spatially autocorrelated training and validation samples inflate performance assessment of convolutional neural networks. ISPRS Open Journal of Photogrammetry and Remote Sensing 5, 100018. https://doi.org/10.1016/j.ophoto.2022.100018.

Kayad, A., Sozzi, M., Gatto, S., Marinello, F., Pirotti, F., 2019. Monitoring Within-Field Variability of Corn Yield using Sentinel-2 and Machine Learning Techniques. Remote Sensing 11, 2873. https://doi.org/10.3390/RS11232873.

Kottek, M., Grieser, J., Beck, C., Rudolf, B., Rubel, F., 2006. World map of the Köppen-geiger climate classification updated. Meteorol. Z. 15, 259–263. https://doi.org/10.1127/0941-2948/2006/0130.

Kuhn, M., 2008. Building predictive models in R using the caret package. J. Stat. Softw. 28. https://doi.org/10.18637/jss.v028.i05.

Kutter, T., Tiemann, S., Siebert, R., Fountas, S., 2011. The role of communication and co-operation in the adoption of precision farming. Precis. Agric. 12, 2–17. https://doi.org/10.1007/s11119-009-9150-0.

Li, L., Wang, B., Feng, P., Wang, H., He, Q., Wang, Y., Liu, D.L., Li, Y., He, J., Feng, H., Yang, G., Yu, Q., 2021. Crop yield forecasting and associated optimum lead time analysis based on multi-source environmental data across China. Agric. For. Meteorol. 308–309, 108558. https://doi.org/10.1016/j.agrformet.2021.108558.
Lingwal, S., Bhatia, K.K., Singh, M., 2022. A novel machine learning approach for rice yield estimation. J. Exp. Theor. Artif. Intell. 1–20. https://doi.org/10.1080/0952813X.2022.2062458.
Liu, B., Martre, P., Ewert, F., Porter, J.R., Challinor, A.J., Müller, C., Ruane, A.C., Waha, K., Thorburn, P.J., Aggarwal, P.K., Ahmed, M., Balkovič, J., Basso, B., Biernath, C., Bindi, M., Cammarano, D., De Sanctis, G., Dumont, B., Espadafor, M., Eyshi Rezaei, E., Ferrise, R., Garcia-Vila, M., Gayler, S., Gao, Y., Horan, H., Hoogenboom, G., Izaurralde, R.C., Jones, C.D., Kassie, B.T., Kersebaum, K.C., Klein, C., Koehler, A.K., Maiorano, A., Minoli, S., Montesino San Martin, M., Naresh Kumar, S., Nendel, C., O'Leary, G.J., Palosuo, T., Priesack, E., Ripoche, D., Rötter, R. P., Semenov, M.A., Stöckle, C., Streck, T., Supit, I., Tao, F., Van der Velde, M., Wallach, D., Wang, E., Webber, H., Wolf, J., Xiao, L., Zhang, Z., Zhao, Z., Zhu, Y., Asseng, S., 2019. Global wheat production with 1.5 and 2.0°C above pre-industrial warming. Glob. Chang. Biol. 25, 1428–1444. https://doi.org/10.1111/GCB.14542.
Liu, Y., Wang, S., Chen, J., Chen, B., Wang, X., Hao, D., Sun, L., 2022. Rice yield prediction and model interpretation based on satellite and climatic indicators using a transformer method. Remote Sens (Basel) 14, 5045. https://doi.org/10.3390/RS14195045/S1.
Lybbert, T.J., Sumner, D.A., 2012. Agricultural technologies for climate change in developing countries: policy options for innovation and technology diffusion. Food Policy 37, 114–123. https://doi.org/10.1016/J.FOODPOL.2011.11.001.
Lynch, J., Cain, M., Frame, D., Pierrehumbert, R., 2021. Agriculture's contribution to climate change and role in mitigation is distinct from predominantly fossil CO2-emitting sectors. Front Sustain Food Syst 4, 300. https://doi.org/10.3389/FSUFS.2020.518039/BIBTEX.
Maestrini, B., Basso, B., 2021. Subfield crop yields and temporal stability in thousands of US midwest fields. Precis. Agric. 22, 1749–1767. https://doi.org/10.1007/s11119-021-09810-1.
Maimoun, M., Madani, K., Reinhart, D., 2016. Multi-level multi-criteria analysis of alternative fuels for waste collection vehicles in the United States. Sci. Total Environ. 550, 349–361. https://doi.org/10.1016/j.scitotenv.2015.12.154.
Masi, M., Di Pasquale, J., Vecchio, Y., Capitanio, F., 2023. Precision farming: barriers of variable rate technology adoption in italy. Land (Basel) 12, 1084. https://doi.org/10.3390/land12051084.
Meroni, M., Waldner, F., Seguini, L., Kerdiles, H., Rembold, F., 2021. Yield forecasting with machine learning and small data: What gains for grains? Agric. For. Meteorol. 308–309, 108555. https://doi.org/10.1016/j.agrformet.2021.108555.
Millard, K., Richardson, M., 2015. On the importance of training data sample selection in random forest image classification: a case study in peatland ecosystem mapping. Remote Sens (Basel) 7, 8489–8515. https://doi.org/10.3390/rs70708489.
Moknatian, M., Piasecki, M., 2019. Lake volume data analyses: a deep look into the shrinking and expansion patterns of lakes azuei and enriquillo. Hispaniola. Hydrology 7, 1. https://doi.org/10.3390/hydrology7010001.
Mongiano, G., Titone, P., Pagnoncelli, S., Sacco, D., Tamborini, L., Pilu, R., Bregaglio, S., 2020. Phenotypic variability in Italian rice germplasm. Eur. J. Agron. 120, 126131. https://doi.org/10.1016/j.eja.2020.126131.
Montero, D., 2021. eemont: a Python package that extends Google Earth Engine. J Open Source Softw 6, 3168. https://doi.org/10.21105/joss.03168.
Montero, D., Aybar, C., Mahecha, M.D., Martinuzzi, F., Söchting, M., Wieneke, S., 2023. A standardized catalogue of spectral indices to advance the use of remote sensing in Earth system research. Sci. Data 10, 197. https://doi.org/10.1038/s41597-023-02096-0.
Murtagh, F., 1991. Multilayer perceptrons for classification and regression. Neurocomputing 2, 183–197. https://doi.org/10.1016/0925-2312(91)90023-5.
Nutini, F., Confalonieri, R., Paleari, L., Pepe, M., Criscuolo, L., Porta, F., Ranghetti, L., Busetto, L., Boschetti, M., 2021. Supporting operational site-specific fertilization in rice cropping systems with infield smartphone measurements and Sentinel-2 observations. Precis. Agric. 22, 1284–1303. https://doi.org/10.1007/s11119-021-09784-0.
Pasuquin, E., Lafarge, T., Tubana, B., 2008. Transplanting young seedlings in irrigated rice fields: early and high tiller production enhanced grain yield. Field Crops Res 105, 141–155. https://doi.org/10.1016/j.fcr.2007.09.001.
Picard, R.R., Cook, R.D., 1984. Cross-validation of regression models. J. Am. Stat. Assoc. 79, 575–583. https://doi.org/10.1080/01621459.1984.10478083.
Pulina, A., Ferrise, R., Mula, L., Brilli, L., Giglio, L., Iocola, I., Ventrella, D., Zavattaro, L., Grignani, C., Roggero, P.P., 2022. The ability of crop models to predict soil organic carbon changes in a maize cropping system under contrasting fertilization and residues management: evidence from a long-term experiment. Ital. J. Agron. 17. https://doi.org/10.4081/ija.2022.2179.
Quinlan, J.R., 1992. Learning with continuous classes. In: 5th Australian joint conference on artificial intelligence, Vol. 92, pp. 343–348.
Ranghetti, L., Boschetti, M., 2022. Updated trends of water management practice in the Italian rice paddies from remotely sensed imagery. Eur J Remote Sens 55, 1–9. https://doi.org/10.1080/22797254.2021.2002726.
Reichardt, M., Jürgens, C., Klöble, U., Hüter, J., Moser, K., 2009. Dissemination of precision farming in Germany: acceptance, adoption, obstacles, knowledge transfer and training activities. Precis. Agric. 10, 525–545. https://doi.org/10.1007/s11119-009-9112-6.
Rigden, A.J., Mueller, N.D., Holbrook, N.M., Pillai, N., Huybers, P., 2020. Combined influence of soil moisture and atmospheric evaporative demand is important for accurately predicting US maize yields. Nat. Food 1, 127–133. https://doi.org/10.1038/s43016-020-0028-7.
Rouse, J.W., Haas, R.H., Schell, J.A., Deering, D.W., 1974. Monitoring vegetation systems in the Great Plains with ERTS. NASA Spec. Publ 351 (1), 309.
Roy, T., George, K.J., 2020. Precision farming: a step towards sustainable, climate-smart agriculture. Global Climate Change: Resilient and Smart Agriculture 199–220. https://doi.org/10.1007/978-981-32-9856-9_10.
Ruan, G., Li, X., Yuan, F., Cammarano, D., Ata-UI-Karim, S.T., Liu, X., Tian, Y., Zhu, Y., Cao, W., Cao, Q., 2022. Improving wheat yield prediction integrating proximal sensing and weather data with machine learning. Comput. Electron. Agric. 195, 106852. https://doi.org/10.1016/j.compag.2022.106852.
Sabo, F., Meroni, M., Waldner, F., Rembold, F., 2023. Is deeper always better? Evaluating deep learning models for yield forecasting with small data. Environ. Monit. Assess. 195, 1153. https://doi.org/10.1007/s10661-023-11609-8.
Sánchez, B., Rasmussen, A., Porter, J.R., 2014. Temperatures and the growth and development of maize and rice: a review. Glob. Chang. Biol. 20, 408–417. https://doi.org/10.1111/gcb.12389.
Schauberger, B., Jägermeyr, J., Gornott, C., 2020. A systematic review of local to regional yield forecasting approaches and frequently used data resources. Eur. J. Agron. 120, 126153. https://doi.org/10.1016/j.eja.2020.126153.
Senapati, N., Stratonovitch, P., Paul, M.J., Semenov, M.A., 2019. Drought tolerance during reproductive development is important for increasing wheat yield potential under climate change in Europe. J. Exp. Bot. 70, 2549–2560. https://doi.org/10.1093/JXB/ERY226.
Shah, S.H., Angel, Y., Houborg, R., Ali, S., McCabe, M.F., 2019. A random forest machine learning approach for the retrieval of leaf chlorophyll content in wheat. Remote Sens (Basel) 11, 920. https://doi.org/10.3390/rs11080920.
Sihi, D., Dari, B., Kuruvila, A.P., Jha, G., Basu, K., 2022. Explainable machine learning approach quantified the long-term (1981–2015) impact of climate and soil properties on yields of major agricultural crops across CONUS. Front Sustain Food Syst 6. https://doi.org/10.3389/fsufs.2022.847892.
Son, N.-T., Chen, C.-F., Chen, C.-R., Guo, H.-Y., Cheng, Y.-S., Chen, S.-L., Lin, H.-S., Chen, S.-H., 2020. Machine learning approaches for rice crop yield predictions using time-series satellite data in Taiwan. Int. J. Remote Sens. 41, 7868–7888. https://doi.org/10.1080/01431161.2020.1766148.
Son, N.-T., Chen, C.-F., Cheng, Y.-S., Toscano, P., Chen, C.-R., Chen, S.-L., Tseng, K.-H., Syu, C.-H., Guo, H.-Y., Zhang, Y.-T., 2022. Field-scale rice yield prediction from Sentinel-2 monthly image composites using machine learning algorithms. Ecol Inform 69, 101618. https://doi.org/10.1016/j.ecoinf.2022.101618.
Stepanov, A., Dubrovin, K., Sorokin, A., Aseeva, T., 2020. Predicting Soybean Yield at the Regional Scale Using Remote Sensing and Climatic Data. Remote Sensing 12, 1936. https://doi.org/10.3390/RS12121936.
Stineman, R.W., 1980. A consistently well-behaved method of interpolation. Creat Comput.
Straffelini, E., Tarolli, P., 2023. Climate change-induced aridity is affecting agriculture in Northeast Italy. Agr. Syst. 208, 103647. https://doi.org/10.1016/J.AGSY.2023.103647.
Subramanian, J., Simon, R., 2013. Overfitting in prediction models – is it a problem only in high dimensions? Contemp. Clin. Trials 36, 636–641. https://doi.org/10.1016/j.cct.2013.06.011.
van Dijk, M., Morley, T., Rau, M.L., Saghai, Y., 2021. A meta-analysis of projected global food demand and population at risk of hunger for the period 2010–2050. Nature Food 2 (7), 494–501. https://doi.org/10.1038/s43016-021-00322-9.
van Klompenburg, T., Kassahun, A., Catal, C., 2020. Crop yield prediction using machine learning: a systematic literature review. Comput. Electron. Agric. 177, 105709. https://doi.org/10.1016/j.compag.2020.105709.
Vance, J.M., Currie, K., Zeldis, J., Dillingham, P.W., Law, C.S., 2022. An empirical MLR for estimating surface layer DIC and a comparative assessment to other gap-filling techniques for ocean carbon time series. Biogeosciences 19, 241–269. https://doi.org/10.5194/bg-19-241-2022.
Vapnik, V., 1998. The support vector method of function estimation. In: Nonlinear modeling: Advanced black-box techniques. Springer US, Boston, MA, pp. 55–85. https://doi.org/10.1007/978-1-4615-5703-6_3.
Vecchio, Y., De Rosa, M., Pauselli, G., Masi, M., Adinolfi, F., 2022. The leading role of perception: the FACOPA model to comprehend innovation adoption. Agric. Food Econ. 10, 5. https://doi.org/10.1186/s40100-022-00211-0.
Veerakachen, W., Raksapatcharawong, M., 2020. RiceSAP: An Efficient Satellite-Based AquaCrop Platform for Rice Crop Monitoring and Yield Prediction on a Farm- to Regional-Scale. Agronomy 10, 858. https://doi.org/10.3390/AGRONOMY10060858.
Wang, F., Huang, J., Tang, Y., Wang, X., 2007. New vegetation index and its application in estimating leaf area index of rice. Rice Sci. 14, 195–203. https://doi.org/10.1016/s1672-6308(07)60027-4.
Weikai, Y., Hunt, L.A., 1999. An equation for modelling the temperature response of plants using only the cardinal temperatures. Ann. Bot. 84, 607–614. https://doi.org/10.1006/anbo.1999.0955.
Whelan, B., Taylor, J., 2013. Precision agriculture for grain production systems. Csiro publishing. https://doi.org/10.1071/9780643107489.
Williams, C.K.I., 1998. Prediction with Gaussian Processes: From Linear Regression to Linear Prediction and Beyond. In: Learning in Graphical Models. Springer, Netherlands, Dordrecht, pp. 599–621. https://doi.org/10.1007/978-94-011-5014-9_23.
Wilson, E.H., Sader, S.A., 2002. Detection of forest harvest type using multiple dates of Landsat TM imagery. Remote Sens. Environ. 80, 385–396. https://doi.org/10.1016/S0034-4257(01)00318-2.
Yang, M., Xu, X., Li, Z., Meng, Y., Yang, X., Song, X., Yang, G., Xu, S., Zhu, Q., Xue, H., 2022. Remote sensing prescription for rice nitrogen fertilizer recommendation based

on improved NFOA model. Agronomy 12, 1804. https://doi.org/10.3390/agronomy12081804.

Yu, Y., Clark, J.S., Tian, Q., Yan, F., 2022. Rice yield response to climate and price policy in high-latitude regions of China. Food Secur. 14, 1143–1157. https://doi.org/10.1007/S12571-021-01253-W/TABLES/11.

Yu, W., Yang, G., Li, D., Zheng, H., Yao, X., Zhu, Y., Cao, W., Qiu, L., Cheng, T., 2023. Improved prediction of rice yield at field and county levels by synergistic use of SAR, optical and meteorological data. Agric. For. Meteorol. 342, 109729. https://doi.org/10.1016/j.agrformet.2023.109729.

Zhang, K., Ge, X., Shen, P., Li, W., Liu, X., Cao, Q., Zhu, Y., Cao, W., Tian, Y., 2019. Predicting rice grain yield based on dynamic changes in vegetation indexes during early to mid-growth stages. Remote Sens. (Basel) 11, 387. https://doi.org/10.3390/rs11040387.

Zhang, H., Zhang, Y., Liu, K., Lan, S., Gao, T., Li, M., 2023. Winter wheat yield prediction using integrated Landsat 8 and Sentinel-2 vegetation index time-series data and machine learning algorithms. Comput. Electron. Agric. 213, 108250. https://doi.org/10.1016/j.compag.2023.108250.